ELSEVIER

Contents lists available at ScienceDirect

Precambrian Research

journal homepage: www.elsevier.com/locate/precamres



Zircon U-Pb ages and Lu-Hf isotopic systematics in granites from Mt Isa Inlier — evidence of prolonged reworking of an active continental margin during the final assembly of the Nuna (Columbia) supercontinent

Sutthida Noptalung *0, Ioan V. Sanislav, Helen A. Cocker, Avish Kumar

Economic Geology Research Centre (EGRU) and Earth and Environmental Science, James Cook University, Townsville 4011 QLD, Australia

ARTICLE INFO

Keywords: Mount Isa inlier North Australian Craton Magmatism Crustal evolution Zircon U-Pb

ABSTRACT

The Mount Isa Inlier, located along the eastern margin of the North Australia Craton (NAC) preserves a long history of intrusive activity linked to the assembly of the Nuna supercontinent. The intrusive rocks in the Inlier formed during six igneous events between ca. 1880 and 1490 Ma. Intrusive rocks in the south-western part of the Inlier (Dajarra region) were previously assigned ages of ca. 1680–1650 Ma without direct U-Pb geochronological constraints. New U-Pb zircon ages from granitic rocks in the Dajarra region reveal intrusive events at ca. 1860 Ma, ca. 1820-1780 Ma, ca. 1710-1690 Ma, and ca. 1670-1650 Ma corresponding to the Kalkadoon, Argylla, Wonga-Burstall and Sybella Igneous Events, respectively. These results indicate that these granites are much older than previously thought and have important implications for intrusive relationships and stratigraphic correlations. Zircon Hf isotopic compositions show negative ϵ Hf_(t) values (+0.0 to -5.5) at ca. 1860 Ma, mixed values (-5.3 to + 8.4) at ca. 1820–1780 Ma, and unradiogenic signatures at ca. 1710–1690 Ma (-8.1 to -0.1)and ca. 1650 Ma (-5.1 to -4.3). These isotopic data indicate that the magmas were generated predominantly by internal reworking of older crust with limited juvenile input. The magmatic belts corresponding to the Kalkadoon and Argylla Igneous Events can be correlated with coeval igneous events in the NAC and the South Australia Craton (SAC) and may have formed in response to a northerly dipping subduction system located along the southern margin of the NAC. The Wonga-Burstall and the Sybella Igneous Events may have formed in response to a westward dipping subduction system developed along the eastern margin of the NAC during the final stages of Nuna assembly. The new geochronological and isotopic data presented here fill in an important gap in the magmatic history of the Mount Isa Inlier and contributes towards a more comprehensive understanding of tectonic activity along the eastern margin of the NAC and the final assembly of the Nuna supercontinent.

1. Introduction

Magmatic belts are linear zones of igneous activity that typically form at plate boundaries due to tectonic activity like subduction, collision or rifting. Felsic magmatic belts are common in orogens and represent a record of tectonic activity that can spread the entire duration of tectonism recorded by an orogen. Thus, studying and understanding the timing, distribution and evolution of magmatic belts in orogens is essential for tectonic and paleogeographic reconstructions (Bonin, 1990; Li et al., 2016; Wyllie, 1988; Zhao et al., 2023). The Mount Isa Inlier, located in northwest Queensland is a Proterozoic orogen along the eastern margin of the North Australian Craton (NAC; Fig. 1a) and preserves a record of tectonic and magmatic activity linked to the final

assembly of the Nuna Supercontinent (e.g. Betts & Giles, 2006; Gibson et al., 2025). Its tectonic evolution is marked by the development of linear magmatic belts over a protracted period between ca. 1880 and 1500 Ma (e.g. Betts et al., 2006; Cocker et al., 2025; Neumann et al., 2009). This makes Mount Isa Inlier ideal for studying tectonic activity related to magmatism in an evolving orogen over prolonged time periods. Similar age magmatic belts have been identified in other Paleoproterozoic cratons including the South Australian Craton (SAC), West Australian Craton (WAC), Antarctica, and North America which reflect global tectonic processes during Nuna assembly. Therefore, the granitoids in the Mount Isa Inlier preserve strong evidence linked to supercontinent assembly in their distribution and genesis as preserved by zircon U-Pb and Lu-Hf records.

E-mail address: sutthida.noptalung@my.jcu.edu.au (S. Noptalung).

^{*} Corresponding author.

Most studies suggest that this prolonged magmatic activity reflects a long-lived subduction system associated with a continental margin setting (Betts et al., 2016; Betts & Giles, 2006; Giles et al., 2002; Zhao et al., 2004) although some studies have suggested that some igneous activity may be related to a mantle plume (e.g. Betts et al., 2009; Oliver et al., 1991). The location of the subduction system linked to the tectonism in Mount Isa Inlier is unclear. Some authors (e.g. Betts & Giles, 2006; Gibson et al., 2025) have proposed a northerly dipping subduction system along the southern margin of the NAC between ca. 1880 and 1760 Ma followed by the Wonga Orogeny (ca. 1750 to 1710 Ma) developed in response to a westerly dipping subduction system along the eastern margin (Korsch et al., 2012; Spence et al., 2021, 2022). Since magmatic belts develop in direct response to tectonic processes, understanding their timing and distribution is essential for correlating magmatic events between various Proterozoic terranes, reconstructing global tectonic processes and paleogeography. For example, the ca. 1880 to 1850 Ma magmatic episode documented in the Kalkadoon-Leichardt Belt (KLB; Figs. 1b and c) of the Mount Isa Inlier is common in other NAC terranes, in the SAC and North America suggesting some form of continuity between the Australian and the North American orogens (e.g. Gibson et al., 2025). In contrast, the ca. 1550-1490 Ma magmatism in the Eastern Fold Belt (EFB; Figs. 1b and c) of the Mount Isa Inlier does not have equivalent magmatic episodes in other NAC terranes or in the SAC suggesting plate reconfiguration and a shift in subduction location and related magmatic activity.

The magmatic belts from the Mount Isa Inlier consist of multiple granitoid intrusions aligned along a north-south trend (Fig. 1c).

Geophysical interpretations (e.g. Spampinato et al., 2015) and recent dating by Olierook et al., (2022) of igneous rocks from deep drill holes from the southern part of Mount Isa Inlier indicate that the magmatic belts occur over a strike length of ~ 700 km. The timing of intrusions from the KLB and EFB is well constrained, and various plutons were assigned to the known magmatic events in the region (Brown et al., 2023; Bultitude et al., 2021; Cocker et al., 2025; Le et al., 2021a; Neumann et al., 2009; Page & Sun, 1998; Withnall, 2019; Wyborn, 1998). In contrast, there has been no dating of intrusions from the southern part of the Western Fold Belt (WFB) and most of the igneous rocks from this area have been attributed to the ca. 1680-1650 Ma Sybella Igneous Event (Connors & Page, 1995; Neumann et al., 2006). Therefore, to construct the geochronological framework, we conducted fieldwork and sample collection in the Dajarra region, the southern part of WFB. In this contribution, we present new zircon U-Pb geochronology and Hf isotope data from granitic intrusions from the southern part of the WFB (Dajarra region) thus filling an important gap in understanding the distribution and age of various intrusive rocks in the inlier. The new findings are discussed in terms of magmatic evolution of the Mount Isa Inlier and the larger geodynamic context including supercontinent assembly and correlations with similar age magmatic events across Proterozoic Australia.

2. Background

2.1. Regional geological setting

The Mount Isa Inlier is part of the North Australia Craton which

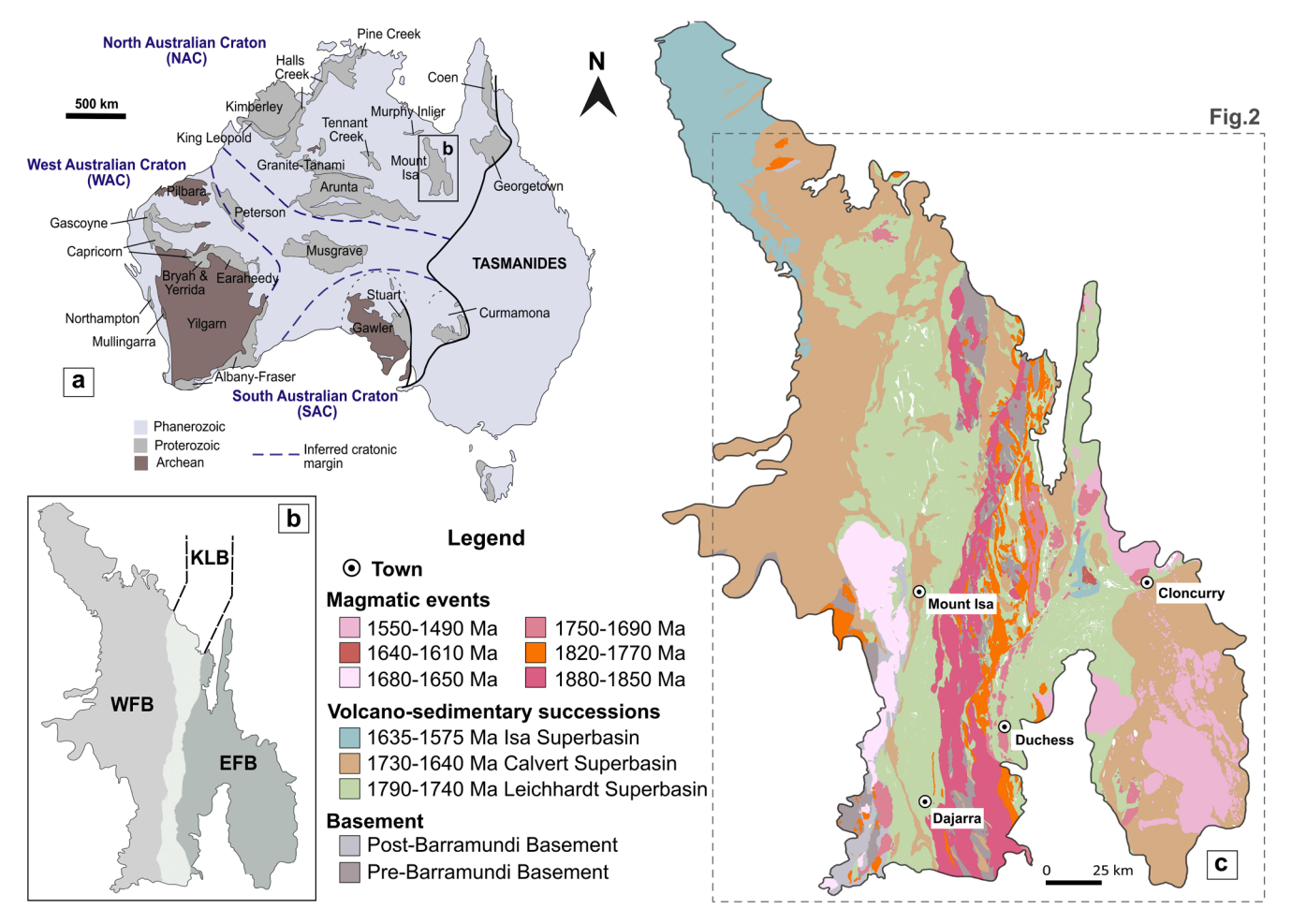


Fig. 1. Mount Isa Inlier located in the North Australian Craton (NAC) (a) was divided into three domains: the Western Fold Belt (WFB), Kalkadoon-Leichhardt Belt (KLB), and Eastern Fold Belt (EFB) (b). Simplified geological map of the inlier showing the distribution of basement rocks, volcano-sedimentary successions related to the three superbasins events, and the magmatic rocks related to the six igneous events (c).

preserves a protracted Paleoproterozoic to Mesoproterozoic evolution spanning from ca. 1870 to 1490 Ma including multiple orogenic and basin forming events (Betts et al., 2006; Blake & Stewart, 1992; MacCready et al., 1998; Scott et al., 2000; Spence et al., 2021, 2022). The Mount Isa Inlier was subdivided into three main tectonostratigraphic components, comprising the EFB, the WFB and the central KLB (Fig. 1b). Furthermore, these three belts have been further subdivided into N-S trending domains based on variations of their geological settings and the presence of bounding structures (Fig. 2a; Geological Survey of Queensland, 2011).

The earliest sequences within the inlier are basement rocks deposited before ca. 1870 Ma (Blake & Stewart, 1992) consisting of a series of units (Kurbayia Metamorphic Complex, Plum Mountain Gneiss, Yaringa Metamorphics, Saint Ronans Metamorphics and Sulieman Gneiss) that are mapped on the geological survey maps as Pre-Barramundi basement and are mainly exposed in the southern region of Mount Isa Inlier. The Pre-Barramundi basement has been deformed and metamorphosed during the ca. 1870–1850 Ma Barramundi Orogeny which is spatially extensive in the North Australia Craton (Bierlein et al., 2008; Etheridge et al., 1987). The Barramundi Orogeny was contemporaneous with

voluminous emplacement of felsic magma and comagmatic volcanic rocks between ca. 1870 and 1850 Ma (Bierlein et al., 2011; Etheridge et al., 1987; Page, 1983; Page & Williams, 1988). This period of magmatism, the Kalkadoon Igneous Event, includes the Kalkadoon Granodiorite and the Ewen Granite as well as the Leichhardt Volcanics cropping out in the Kalkadoon-Leichhardt Belt. The emplacement of felsic magma during ca. 1870–1850 Ma is likely related to a magmatic arc setting during the amalgamation of the North Australian Craton (Bierlein et al., 2011; McDonald et al., 1997).

A series of bimodal volcanics and sedimentary successions from the Mount Isa Inlier have been mapped on the geological survey maps as Post-Barramundi basement with ongoing debate surrounding the timing of metamorphism, deformation and their stratigraphic position (Withnall & Hutton, 2013). These include the pre 1800 Ma volcanosedimentary successions between ca. 1857 Ma (e.g., the Oroopo Metabasalt; Magee et al., 2012) and ca. 1823 Ma (e.g. the Bucket Hole Metavolcanic; Carson et al., 2009). This period ends with the emplacement of the ca. 1810 to 1795 Ma, Big Toby pluton (Carson et al., 2011; Withnall & Hutton, 2013; Wyborn et al., 1988). Zircon age dating suggests that granites of similar age can be found in the southern part of the

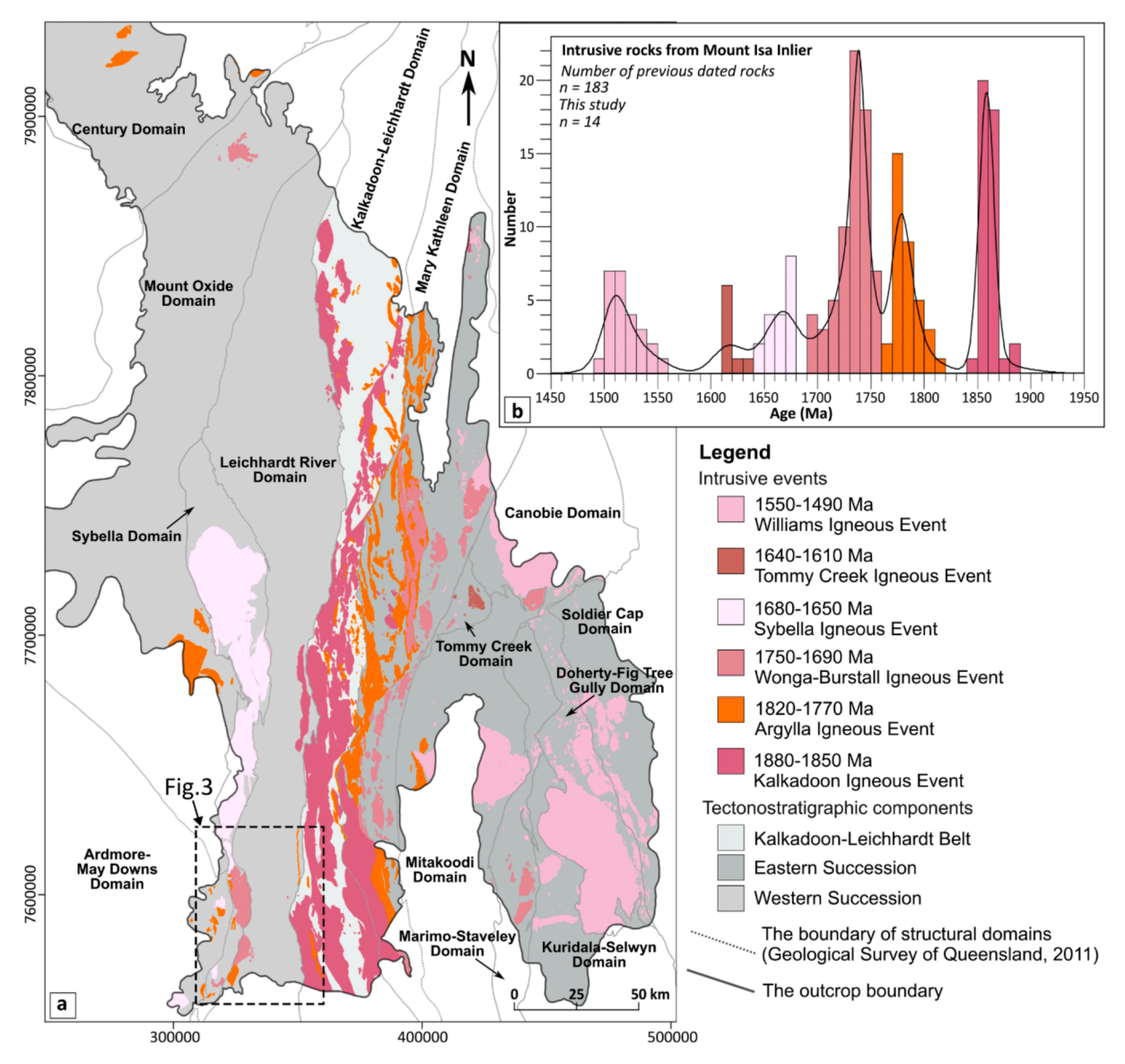


Fig. 2. (a) Simplified geological map focused on the distribution of magmatic events in Mount Isa Inlier and the location of Dajarra region with a square demonstrated in Fig. 3. (b) Probability density distribution and histogram complied from previously published U-Pb ages of intrusive rocks across the Inlier, combined with new dating results from this study (Published age data has been provided in Supplementary material).

exposed Mount Isa Inlier (Magee et al., 2012) and undercover (Olierook et al., 2022).

The major volcano-sedimentary successions deposited between ca. 1800 and 1575 Ma were classified as the Western Succession (WS) in the Western Fold Belt (WFB) and the Eastern Succession (ES) in the Eastern Fold Belt (EFB). They were further subdivided in three distinctive superbasins separated by unconformities and interpreted to represent episodes of continental rifting in a back-arc setting of a complex subduction system occurring either along the southern or the eastern margin of the North Australian Craton (Blake & Stewart, 1992; Cawood & Korsch, 2008; Foster & Austin, 2008; Giles et al., 2002; Iaccheri, 2019; Scott et al., 2000). The three superbasin events include the ca. 1790-1740 Ma Leichhardt Superbasin, the ca. 1730-1640 Ma Calvert Superbasin and the ca. 1635-1575 Ma Isa Superbasin (Gibson et al., 2016). Furthermore, these basin-forming events were interpreted to be coeval with significant magmatism, including the Argylla Igneous Event from ca. 1780 to 1770 Ma, the Wonga-Burstall Igneous Event from ca. 1750 to 1720 Ma, the Weberra Granite at ca. 1710 Ma, and the Sybella Igneous Event from ca. 1680 to 1650 Ma (Withnall & Hutton, 2013; Wyborn et al., 1988).

Following the Barramundi Orogeny, two periods of orogenic events were proposed, the ca. 1750–1710 Ma Wonga Orogeny (Spence et al., 2021, 2022) and the ca. 1650–1490 Ma Isan Orogeny (Abu Sharib & Sanislav, 2013; MacCready et al., 1998; O'Dea et al., 1997b). A compressive event between ca. 1800 and 1770 Ma was documented from the Tick Hill region, but the full extent and its regional significance is not yet known (Le et al., 2021b, 2024). The onset of the Wonga Orogeny coincides with the cessation of sedimentation during the Leichhardt Superbasin, and it appears that the deformation and metamorphism during this orogenic event was most intense in the EFB (Betts, 1999; Blaikie et al., 2017; Spence et al., 2021, 2022; Wilson, 1975). The Isan Orogeny affected the entire inlier and resulted in the reactivation of previous structures and the cessation of sedimentation in the region (Abu Sharib & Sanislav, 2013; Connors & Page, 1995; Gibson et al., 2016; O'Dea et al., 1997b). The final stages of the Isan Orogeny coincide

with the emplacement of voluminous I-type magmatism with A-type affinities, the Williams Igneous Event, in the EFB between ca. 1550–1490 Ma (Page & Sun, 1998).

2.2. Geological setting of Dajarra region

The Dajarra region lies in the southwestern part of the Mount Isa Inlier and consists of four distinct geological domains from west to east; the Ardmore-May Downs domain, the Sybella domain, the Leichhardt River domain, and the Kalkadoon-Leichhardt domain (Fig. 2a; Geological Survey of Queensland, 2011). The eastern boundary of the Dajarra region is the Dajarra fault in the Kalkadoon-Leichhardt domain. The Ardmore-May Downs domain primarily consists of basement rocks, whereas the Leichhardt River and Kalkadoon-Leichhardt domains predominantly comprise metasedimentary rocks attributed to the Western Succession.

Basement rocks in the Dajarra region (Fig. 3a) consist of the Saint Ronans Metamorphics, the Sulieman Gneiss and the Kalkadoon Granodiorite and preserve a complex deformation and metamorphic history (Bultitude, 1982). Additionally, a series of units (the Oroopo Metabasalt, Bucket Hole Metavolcanics, Kallala Quartzite and Alpha Centauri Metamorphics) that predate the Leichardt Superbasin occur mainly in the western part of the Dajarra region and are commonly interpreted as Post-Barramundi basement (Withnall & Hutton, 2013). Historically, these units were mapped as part of the Haslingden Group and interpreted to be deposited coeval to the Leichhardt Superbasin (Blake et al., 1982, 1984; Bultitude, 1982). However, recent studies using U-Pb zircon dating have constrained the sedimentation and volcanic activity of these units between ca. 1850-1820 Ma (Carson et al., 2009; Magee et al., 2012). The metamorphic grade ranges between greenschist and amphibolite facies (Blake et al., 1984) but the timing of deformation and metamorphism is unclear.

Most metasedimentary rocks from the Dajarra region (Fig. 3a) were interpreted to be deposited during the formation of Leichhardt and Calvert Superbasins. The units deposited during the opening of

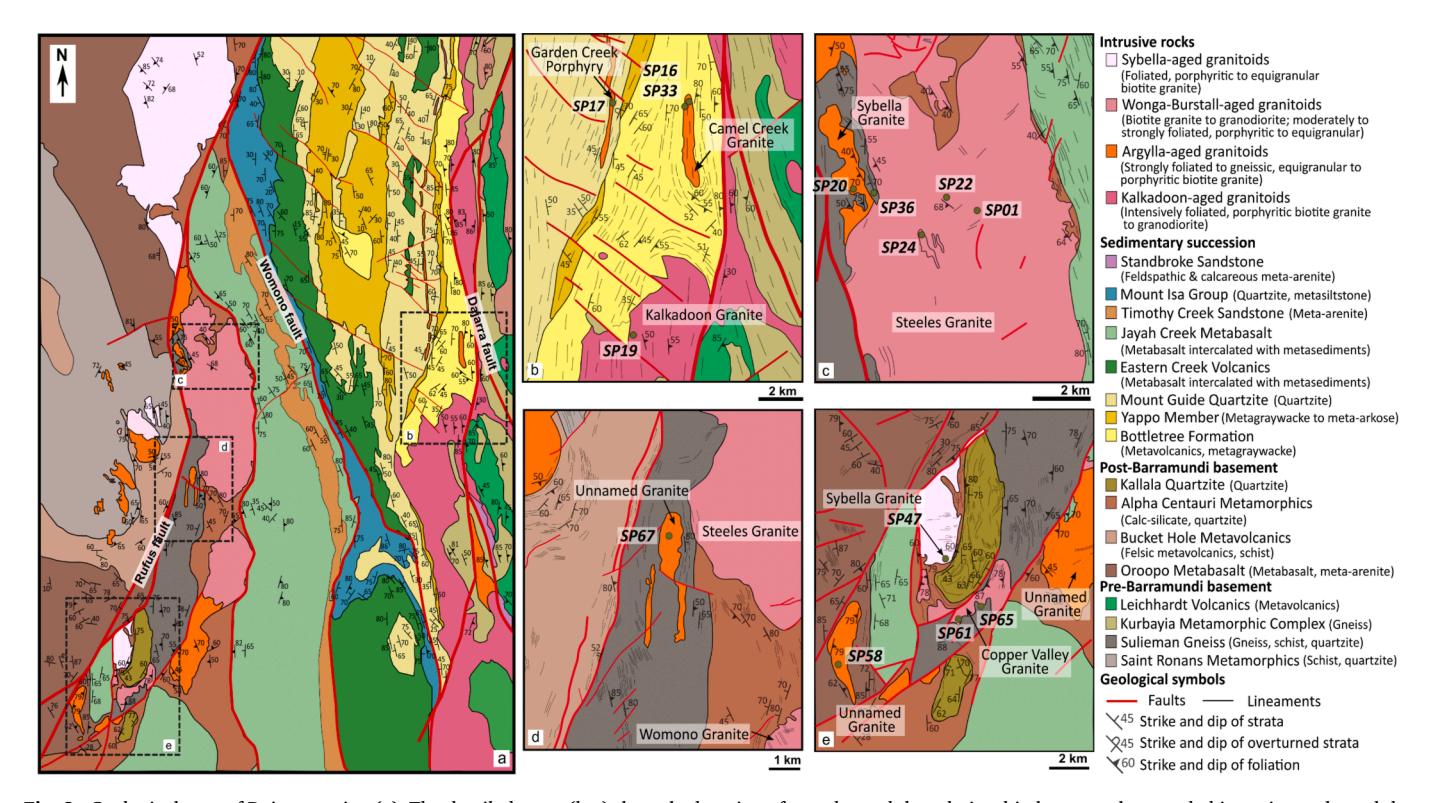


Fig. 3. Geological map of Dajarra region (a). The detailed maps (b-e) show the location of samples and the relationship between the sampled intrusive rocks and the surrounding country rocks.

Leichhardt Superbasin belong to the Bottletree Formation and the Lower Haslingden Group. The Lower Haslingden Group consists of the Yappo Member, Mount Guide Quartzite, Eastern Creek Volcanics, Jayah Creek Metabasalt and the Timothy Creek Sandstone Member. They were interpreted to indicate syn-rift volcanics and rift-related sediments deposited in a fluvial to lacustrine environment (Eriksson & Simpson, 1993; Jackson et al., 2000; Neumann et al., 2006). The Bottletree Formation and the Haslingden Group were mapped as continuous units extending for more than 600 km from the northern part of the inlier to the southernmost margin of the inlier and extending undercover until the Cork Fault (e.g. Spampinato et al., 2015). The succession substantially thickened in the Dajarra region compared to the northern part (Blake, 1987; Bultitude, 1982; Spampinato et al., 2015). Rocks of the Calvert Superbasin are represented by metasediments of the Warrina Park Quartzite and the Moondarra Siltstone which occur as a north--south trending narrow zone surrounded by Haslingden Group rocks on both sides. They are interpreted to indicate marine siliciclastic sedimentation, ranging from shoreface to shallow marine deposits and are metamorphosed to lower greenschist facies (Foster & Rubenach, 2006).

The metasediments of the Dajarra region are intruded mainly by plutons and dykes mapped as belonging to the Sybella Igneous Event and minor intrusions of the Kalkadoon and Wonga-Burstall Igneous Events (Fig. 3a). All intrusions occurring on the western side of the Dajarra region are mapped as belonging to the Sybella Igneous Event. The largest of these intrusions is the Steeles Granite. In the eastern side, a large intrusion mapped as Kalkadoon Granodiorite is in uncertain contact with rocks mapped as the Bottletree Formation. In the north-eastern corner of the region, the Bottletree Formation is intruded by a north–south trending granite, the Camel Creek Granite which is mapped as part of the Wonga-Burstall Igneous Event. The Mount Guide Quartzite is intruded by a long and narrow ~ north–south trending porphyritic dyke, the Garden Porphyry Dyke, mapped as part of the Sybella Igneous Event.

2.3. Magmatic events in Mount Isa Inlier

A compilation of U-Pb zircon ages of intrusive rocks from the Mount Isa Inlier reveals almost 400 Ma of episodic magmatic activity that can be subdivided into six magmatic events occurring between ca. 1870 and 1490 Ma (Fig. 2b). The map pattern shows that these intrusive events occur as approximately north–south trending belts and occupy distinct age and structural domains (Fig. 2a).

The earliest intrusive event, the Kalkadoon Igneous Event, occurs between ca. 1870 and 1850 Ma and is represented by the Kalkadoon-Ewen Batholith which occurs mainly in the Kalkadoon Leichhardt Belt (Fig. 2a). Zircon dating in this research indicates that similar age intrusive rocks occurred further west and intruded into the Sulieman Gneiss (Fig. 3b). The Kalkadoon Igneous Event forms a continuous north-south trending belt of intrusive rocks that is ~ 300 km long and most likely extends further undercover to the north and south of the exposed area. This is followed by a gap of \sim 40 Ma until the intrusion of the Yeldham and Big Toby Granites at ca. 1810 Ma (Wyborn et al., 1988) and the initiation of the Argylla Igneous Event. The Argylla Igneous Event, new name/event proposed by Bultitude et al. (2021) and Cocker et al. (2025), occurs between ca. 1810 and 1770 Ma (Fig. 2b) and consists of three sub-parallel trends of plutons and porphyry dykes (Fig. 2a). The first trend occurs in the Eastern Succession and consists of a series of isolated plutons located mainly within the Mary Kathleen Domain. The second trend occurs only in the southern part of the inlier, in the Dajarra region, represented by the Paper Tank Microgranite. The third trend is located entirely in the Western Succession and includes the Yeldham and Big Toby Granites as well as a series of unnamed intrusive rocks in the south-western corner of the Dajarra region (Fig. 2a).

The third intrusive event, the Wonga-Burstall Intrusive Event, occurred between ca. 1750 and 1690 Ma (Fig. 2b) and consists of three subparallel north-south trends (Fig. 2a). The first trend occurs east of the Mitakoodi Domain and consists of the Gin Creek Granite and the

Levian Granite. The second trend occurs mainly in the Mary Kathleen Domain and consists of a series of intrusives starting from the Tick Hill area in the south to Mount Godkin Granite in the north. The third trend occurs in the Western Succession and consists of the Weberra Granite in the north, the Steeles Granite in the Dajarra region and a few unnamed granites in the south-western area of the Dajarra region included in this research (Fig. 2a). The fourth intrusive event, the Sybella Igneous Event, occurred between ca. 1680 and 1650 Ma (Fig. 2b). Most intrusions associated with this event are in the Western Succession except the Tommy Creek Microgranite located in the Tommy Creek Domain and the Ernest Henry Diorite located in the Canobie Domain (Fig. 2a). The fifth intrusive event, the Tommy Creek Igneous Event, occurred between ca. 1640 and 1610 Ma (Fig. 2b; Brown et al., 2023) and is found only in the Tommy Creek Domain (Fig. 2a). Within the Eastern Succession, this igneous event consists mainly of porphyritic intrusions with minor amounts of granite. The sixth igneous event, the Williams Igneous Event, occurred between ca. 1550 and 1490 Ma (Fig. 2b) and is located in the Eastern Succession forming a north-south belt of large plutons restricted to the southern part of the inlier (Fig. 2a).

3. Methodology

3.1. Sampling

This study is based on samples collected from intrusive units cropping out in the Dajarra region. The sampling strategy involved sampling all major intrusive units from the area that were not previously dated as well as sampling variations within individual intrusive units. Only the least altered samples, with no veins and no visible enclaves of other material were sampled. From each sampling site about 3–4 kg of rock was collected.

3.2. Zircon u-pb dating

All samples were prepared and analysed at James Cook University, Townsville. Zircon grains were obtained using standard crushing methods and the Wilfley table technique. Subsequently, all zircons were handpicked and mounted in epoxy discs, which were then polished to expose the zircons for analysis. The zircon standard GJ1 was used as the primary standard. GJ1 has an ID-TIMS $^{207}\text{Pb}/^{206}\text{Pb}$ age of 608.5 ± 0.4 Ma (Jackson et al., 2004) and a TIMS $^{206}\text{Pb}/^{238}\text{U}$ age of 601.7 ± 0.37 Ma (Horstwood et al., 2016). Additionally, four secondary standards were utilized during the analysis: 91,500 (ID-TIMS $^{207}\text{Pb}/^{206}\text{Pb}$ age = 1065.4 \pm 0.3 Ma; Wiedenbeck et al., 1995), FC1 ($^{207}\text{Pb}/^{206}\text{Pb}$ age = 1099.0 \pm 0.6 Ma; Paces and Miller, 1993), Plešovice (TIMS $^{207}\text{Pb}/^{206}\text{Pb}$ age = 337.96 \pm 0.61 Ma; Sláma et al., 2008), and Temora-2 (TIMS $^{206}\text{Pb}/^{238}\text{U}$ age = 416.8 \pm 0.3 Ma; Black et al., 2003; Tichomirowa et al., 2019). Furthermore, the NIST 610 and 612 reference glass were analysed at the beginning and the end of the run to monitor instrument stability.

Zircon grains were analysed for U-Pb dating at the Advanced Analytical Centre (AAC), James Cook University. All zircons were imaged with a Hitachi SU5000 FE-SEM and cathodoluminescence images were collected to investigate growth zoning and the presence of inherited cores. The cathodoluminescence images informed the selection of the laser ablation sites to ensure that analyses were performed on the same growth domain. Selected grains were analysed by LA-ICP-MS technique (Thermo Scientific iCAP RQ-ICP-MS connected to a Teledyne Photon Machines Analyte G2 Laser) to obtain U-Pb isotope composition. Each analysis started with 30-second blank gas measurement followed by an analysis time of 30 s using a spot size of 25 or 30 μm, 5 Hz repetition rate, and 3 J/cm² energy density. Zircon standards were analysed repeatedly after every 10 unknown zircon analyses to ensure data quality and consistency. For igneous samples, 70-80 magmatic zircons with a range of morphologies and cathodoluminescence responses were analysed to determine the magmatic crystallization ages. The Iolite package (Paton et al., 2011) was utilised

to process data, and the results were displayed by using IsoplotR (Vermeesch, 2018). The 207 Pb/ 206 Pb age and a discordance limit of 10 % were used to calculate the weighted average age. The age of magmatic crystallization was determined by either using the weighted mean or the upper intercept of a discordia line when the sample lacked sufficient concordant grains for calculating weighted mean age.

3.3. Zircon Lu-Hf isotopic data

For Lu-Hf isotopic data acquisition, the analytical procedures followed those outlined by Kemp et al. (2009a). The Hf isotope compositions were acquired using a Thermo-Scientific Neptune MC-ICP-MS coupled with a Teledyne Photon Machines Analyte G2 laser ablation system. Analyses targeted the same zircon areas previously dated by LA-ICP-MS, or the same growth domains defined by cathodoluminescence (CL) imaging. The laser spot size was 50 μm , operating at a repetition rate of 4 Hz.

Reference zircons used in this study included Mud Tank (MTZ) and FC1, with FC1 specifically used to monitor the correction of isobaric interferences from Yb. The Mud Tank zircon was used as primary reference with a $^{176}\mathrm{Hf}/^{177}\mathrm{Hf}$ ratio of 0.282507 ± 0.000006 (Woodhead & Hergt, 2005). The measured average $^{176}\mathrm{Hf}/^{177}\mathrm{Hf}$ value for MTZ during the analytical session was 0.282495 ± 0.000014 , which falls within analytical uncertainty of the accepted value. This result yielded a normalization factor of 1.000042, which was applied to both the FC1 reference zircon, and the unknown samples analysed in this study. After normalization, the average $^{176}\mathrm{Hf}/^{177}\mathrm{Hf}$ value for FC1 was 0.282182 ± 0.000012 . Epsilon hafnium (eHf) values were calculated using the present-day chondritic uniform reservoir (CHUR) values of $^{176}\mathrm{Hf}/^{177}\mathrm{Hf}=0.282785$ and $^{176}\mathrm{Lu}/^{177}\mathrm{Hf}=0.0336$ (Bouvier et al., 2008). Initial $^{176}\mathrm{Hf}/^{177}\mathrm{Hf}$ ratios were determined using a $^{176}\mathrm{Lu}$ decay constant of $1.867\times10^{-5}\,\mathrm{My}^{-1}$ (Söderlund et al., 2004).

4. Results

4.1. Kalkadoon Igneous Event (1880-1850 Ma)

4.1.1. Sample SP19 - Kalkadoon Granite

This sample is from a north-south trending porphyritic granodiorite intrusion along the contact between the Bottletree Formation and the north-western margin of a large intrusion mapped as part of the Kalkadoon Granodiorite (Fig. 3b and Fig. 4a). The larger intrusion is foliated, fine to medium grained and consists of quartz, feldspars and biotite. The porphyritic intrusion does not display a clear foliation although on some surfaces a weakly developed alignment of minerals can be identified. The groundmass is medium to coarse grained and consists of quartz, feldspar and biotite whereas the porphyritic appearance is given by undeformed, 2-3 cm long, pink potassic feldspars. The Bottletree formation consists of an intercalation of folded and foliated quartzite, mica schist, metasiltstone and metaconglomerate. The formation is folded around north-south trending axes, and the folded layers are truncated on the map pattern by the smaller porphyritic and the larger intrusion. The direct contact between the two granitic intrusions and the Bottletree Formation is not exposed but indirect field observations are consistent with the mapped pattern.

Zircon grains separated from sample SP19 have euhedral to subhedral shapes and range in colour from brown to colourless. Cathodoluminescence (CL) images reveal that most grains have low luminescence, with zones of higher luminescence found only in some grains as a concentric rim or irregular shaped zones around the rim. Most analyses are highly discordant and have experienced lead loss. Twenty-nine zircon grains form a well-defined discordia line with an upper intercept age of 1860 \pm 6 Ma (Fig. 5a) whereas twenty-two of these zircons have concordant ages yielding a $^{207}\text{Pb/}^{206}\text{Pb}$ weighted average age of 1856 \pm 6 Ma (Fig. 5b). The two ages are identical within uncertainty $^{207}\text{Pb/}^{206}\text{Pb}$ weighted average age of 1856 \pm 6 Ma is

interpreted as the emplacement age for the Kalkadoon Granodiorite at this location.

4.1.2. Sample SP36 - Sulieman Gneiss

The Sulieman Gneiss is poorly exposed and most outcrops in the region consist of quartzite and amphibolite. A quartzofeldspathic rock with a gneissic texture, mapped as the Sulieman Gneiss, crops along the road-cutting on the Boulia–Mount Isa Highway (Fig. 3c). Sample SP36 was collected from this road cut (Fig. 4b). The sample consists of deformed and aligned quartz, feldspar (plagioclase > microcline) and muscovite (probably after biotite) defining a gneissic foliation trending north south and dipping steeply ($\sim\!70^\circ$) west. The homogenous composition and texture of this gneissic rock suggest that the most likely protolith is granite. The relationship between this quartzofeldspathic gneiss and the surrounding rocks could not be defined due to the lack of outcrops.

Zircons grains separated from sample SP36 generally prismatic shaped, euhedral and vary in colour from brown to colourless. CL images reveal that most grains have oscillatory growth zoning with evidence of metamictization present in some grains. Sixteen zircon grains yield an upper concordia intercept age of 1855 \pm 6 Ma (Fig. 5c) and form a single cluster with a weighted average $^{207}\text{Pb}/^{206}\text{Pb}$ age of 1854 \pm 6 Ma (Fig. 5d), which is interpreted to represent the best estimate for the crystallization age of this gneissic rock.

4.2. Argylla Igneous Event (1820-1770 Ma)

4.2.1. Sample SP16 and SP 33 - Camel Creek Granite

The Camel Creek Granite is an \sim 4 km long and 400 m wide intrusion in the Bottletree Formation (Fig. 3b). It was previously assigned to the Wonga-Burstall Igneous Event, but our dating indicated that it belongs to the Argylla Igneous Event. The intrusion contains a well-developed, north south trending subvertical foliation similar to the main structural trend including the axial planar foliation of the folds in the surrounding Bottletree Formation. Along the margin of the intrusion the deformation is more intense and a mylonitic fabric is well developed (Fig. 4c). This was particularly well developed on the eastern side of the intrusion. On the western side of the intrusion enclaves of the surrounding Bottletree Formation are more common compared to the eastern side. The granite is medium grained, equigranular, and the mineralogy is dominated by quartz, feldspars and micas. Sample SP16 was collected from the less deformed part of the intrusion whereas sample SP33 was collected from the mylonitic granite along the eastern margin of the intrusion.

Zircon grains separated from sample SP16 are mainly subhedral with euhedral grains being less common and vary in colour from brown to transparent. The CL images reveal concentric zoning with moderate luminescence cores surrounded by higher luminescence concentric zones towards the rim. Thirteen zircon grains define a discordia line with an upper concordia intercept age of 1806 \pm 13 Ma (Fig. 5e) whereas eight concordant grains yield a $^{207} \rm Pb/^{206} Pb$ weighted average age of 1801 \pm 12 Ma (Fig. 5f) which is interpreted as the emplacement age for this granite.

Zircon grains separated from sample SP33 are transparent in colour and have subhedral to euhedral shapes. Cathodoluminescence imagining reveals that zircons grains from this sample have a variety of internal structures ranging from thin concentric growth zoning to wide planar growth zones to grains that display no zoning. Most grains separated from this sample are concordant. Eighty-nine of these grains define a discordia line with an upper intercept age of 1785 \pm 3 Ma (Fig. 5g) whereas eighty-six analyses yield $^{207}\text{Pb}/^{206}\text{Pb}$ weighted average age of 1784 \pm 3 Ma (Fig. 5h), which is interpreted as the magmatic crystallization age for this mylonitic granite.

4.2.2. Sample SP17 – Garden Creek Porphyry

The Garden Creek Porphyry, previously assigned to the Wonga-

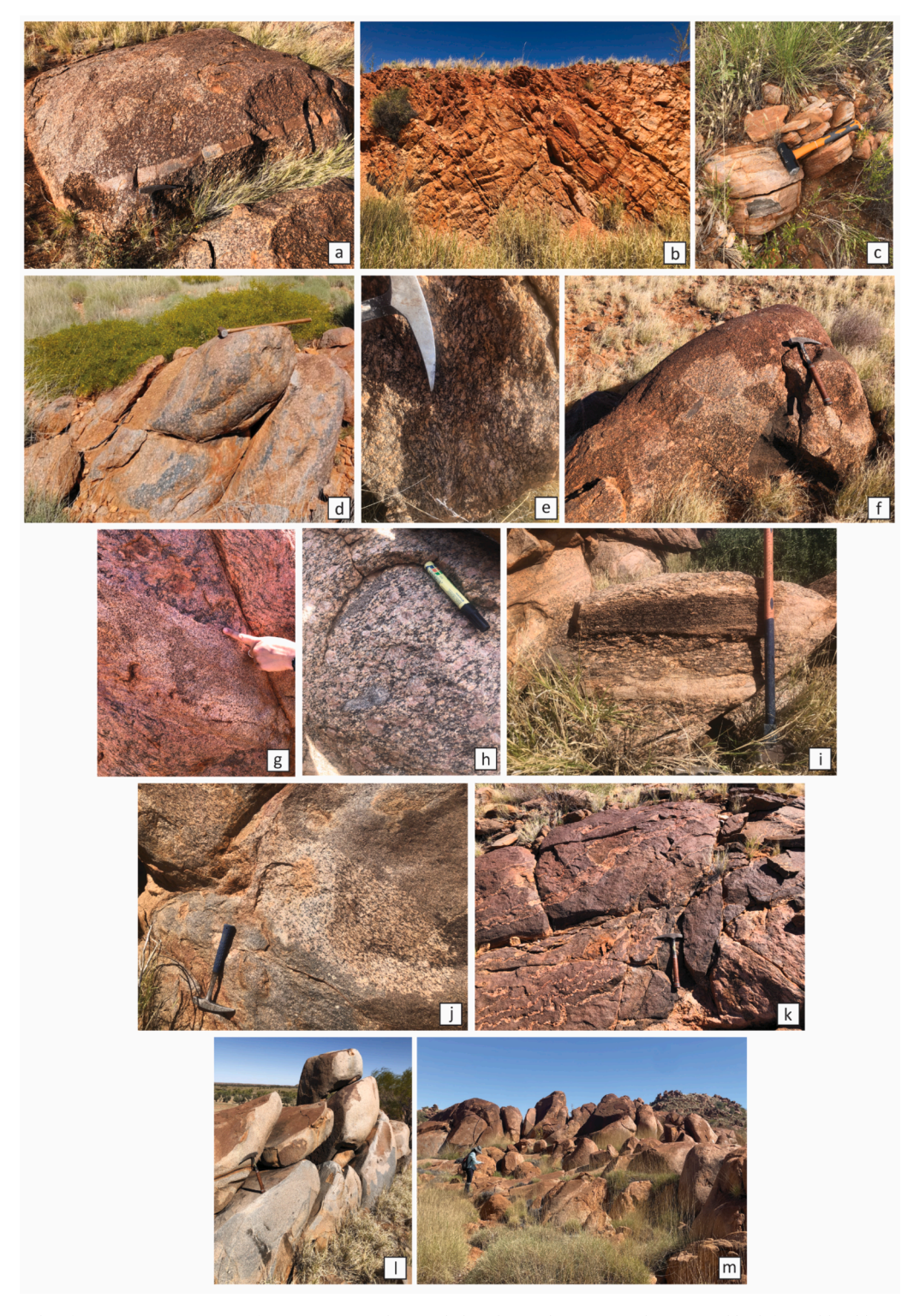


Fig. 4. Field photographs of representative outcrops from intrusive rocks sampled in this study: (a) a porphyritic weakly deformed bouldery outcrop of Kalkadoon Granite (SP19); (b) quartzofeldspathic gneiss from the Sulieman Gneiss outcropping along the road cut (SP36); (c) mylonitic Camel Creek Granite at the contact with the Bottletree Formation (SP33); (d) bouldery outcrop of undeformed, porphyritic Garden Creek Porphyry (SP17); (e) gneissic granite of an unnamed intrusive unit (SP20); (f) foliated bouldery outcrop of unnamed granite containing mafic enclaves aligned with the regional strain fabric (SP58); (g) strongly foliated to gneissic unnamed granite cut by a later granitic dyke (SP67); (h) porphyritic biotite granite with mafic enclaves from the central part of the Steeles Granite (SP01); (i) strongly foliated porphyritic biotite granite from the margin of the Steeles Granite (SP22); (j) foliated porphyritic granite intruding strongly foliated granodiorite (SP24) within the Steeles Granite; (k) migmatitic Copper Valley Granite (SP61); (l) unnamed felsic intrusive adjacent to the Copper Valley Granite (SP65); (m) bouldery outcrops of Sybella Granite (SP47).

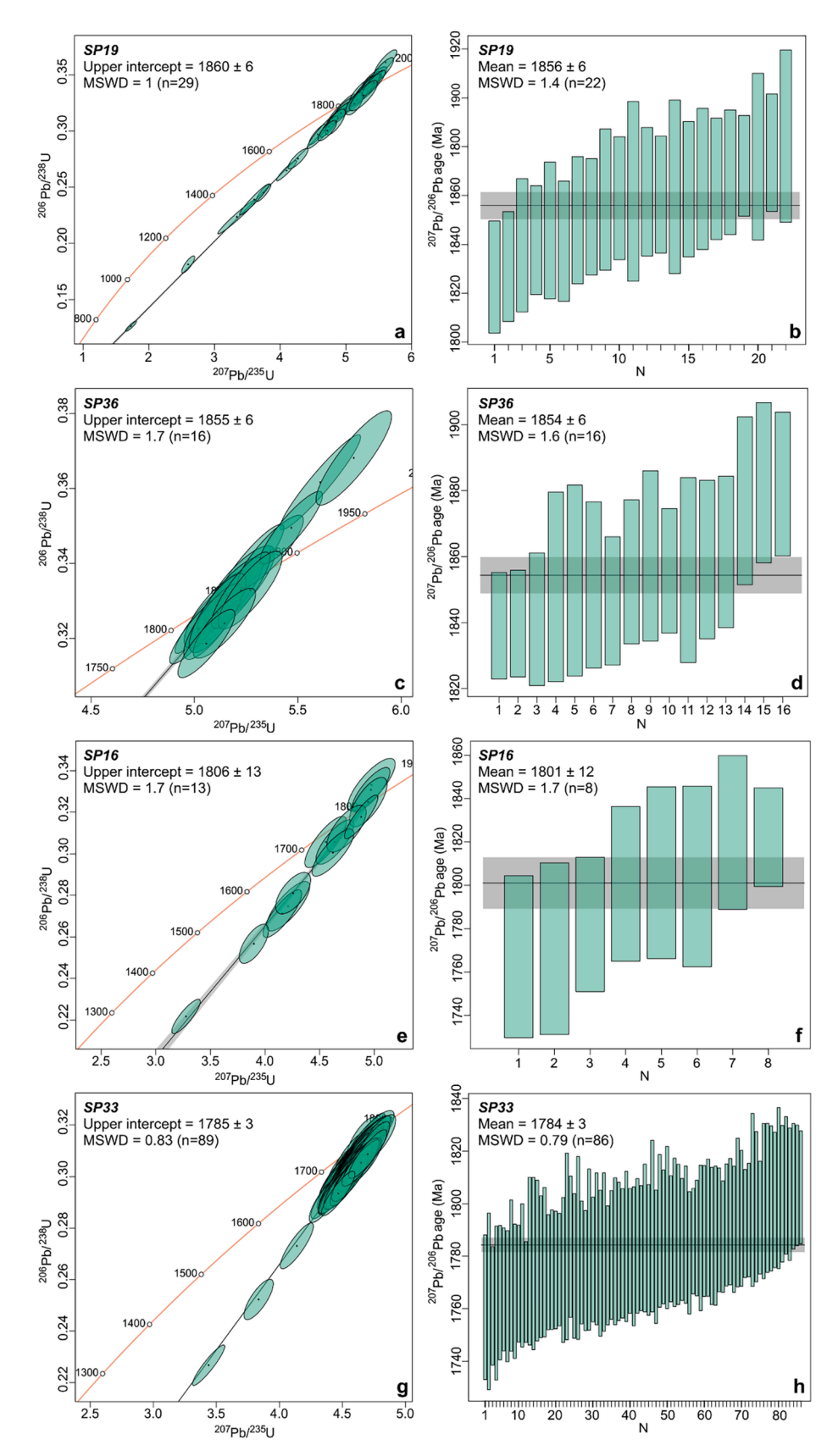


Fig. 5. U-Pb zircon data from magmatic zircons of the Kalkadoon Igneous Event (SP19 and SP36) and the Argylla Igneous Event magmatic event (SP16 and SP33). The results are illustrated as an upper intercept age on concordia plots and as weighted average ages.

Burstall Igneous Event, is a $\sim37~km$ long and 100 to 250 m wide, north south trending dyke that intrudes the Mount Guide Quartzite (Fig. 3b). Sample SP17 was collected from the southern part of the Garden Creek Porphyry $\sim7~km$ north of Dajarra town. The dyke is sub-vertical and crosscuts the layering and foliation in the Mount Guide Quartzite (Fig. 4d). It is undeformed, dark grey and consists of centimetre size potassic feldspar crystals in a medium to fine grained matrix of quartz, feldspar and biotite.

Zircon grains from sample SP17 are euhedral to subhedral shaped and brown to colourless under the binocular microscope. They have concentric growth zoning with low to medium luminescence cores surrounded by higher luminescence rims. Forty-three analyses define a discordia line with an upper concordia intercept age of 1783 \pm 5 Ma (Fig. 6a) that is identical to the $^{207}\text{Pb}/^{206}\text{Pb}$ weighted average age of 1783 \pm 5 Ma (Fig. 6b) obtained from thirty-six concordant grains and interpreted as the emplacement age for the Garden Creek Porphyry. Additionally, eleven concordant analyses yielded a $^{207}\text{Pb}/^{206}\text{Pb}$ weighted average age of 1827 \pm 10 Ma and are interpreted as inherited grains (Table 1).

4.2.3. Sample SP20 - Sybella Granite

Sample SP20 has been collected from a pluton mapped as Sybella Granite, but our dating indicates that this pluton belongs to the Argylla Igneous Event. It was collected from the southern part of a pluton that occurs in the northwestern part of the Dajarra region (Fig. 3c). The pluton consists of two separate intrusions. A larger one, in the northern part, that intrudes into the Alpha Centauri Metamorphics, the Sulieman Gneiss and is cut on the western side by the Rufus Fault; and a smaller one, in the southern part, that intrudes only in the Sulieman Gneiss. This pluton is strongly foliated to gneissic, and its grain size varies from medium grained to coarse grained to porphyritic (Fig. 4e). It is mainly granodioritic in composition consisting of quartz, feldspar biotite and hornblende; locally grading into leucogranite.

Zircon grains from sample SP20 have euhedral to subhedral shapes with elongate morphologies and are translucent and colourless. CL images reveal that most grains have concentric growth zoning with low to medium luminescence cores surrounded by higher luminescence zones towards the rim. There are also a few metamict grains. Twenty-six zircon grains define a discordia line with an upper concordia intercept age of 1783 ± 5 Ma (Fig. 6c) which is identical, within uncertainty, to the $^{207}\text{Pb}/^{206}\text{Pb}$ weighted average age of 1782 ± 6 Ma (Fig. 6d) obtained from 19 concordant grains and interpreted as the emplacement age for this granite.

4.2.4. Sample SP58 and SP67 - Unnamed Granite

Sample SP58 was collected from intrusive bodies located in the southwestern part of the Dajarra region whereas sample SP67 was collected from an intrusion located south of the Steeles Granite. These intrusions are not named on geological maps but have been assigned to the Sybella Igneous Event. Our dating indicates that they belong to the Argylla Igneous Event.

Sample SP58 is from a granitic pluton that intruded in the Oroopo Metabasalt (Fig. 3e). It is mainly composed of equigranular to porphyritic, foliated biotite granite and locally is grading into granodiorite and diorite. Deformed xenoliths and mafic enclaves are common within the pluton (Fig. 4f).

Zircon grains from sample SP58 are translucent with colour ranging from colourless to brown, and euhedral with needle-like shapes. Most zircon grains exhibit low to moderate luminescence with visible concentric zoning. Fifty-five analyses define a discordia line with an upper concordia intercept age of 1786 \pm 4 Ma (Fig. 6e), which is identical, within uncertainty, to the $^{207}\text{Pb}/^{206}\text{Pb}$ weighted average 1787 \pm 4 Ma (Fig. 6f) obtained from forty-seven concordant analyses. The 1787 \pm 4 Ma $^{207}\text{Pb}/^{206}\text{Pb}$ weighted average age is interpreted to represent the emplacement age for this granite. Moreover, eleven concordant analyses form a single population with a $^{207}\text{Pb}/^{206}\text{Pb}$

weighted average age of 1829 ± 9 Ma (Table 1), which is interpreted to represent inherited zircon grains.

Sample SP67 was collected from a small, north south trending, granitic pluton intruding the Sulieman Gneiss (Fig. 3d). The granite is strongly foliated, displaying a gneissic texture and contains minor amounts of augen gneiss (Fig. 4g).

Zircon grains extracted from sample SP67 are euhedral to subhedral with elongated shapes and vary in colour from semi-translucent to yellowish to brown. Twenty-four zircon grains define a discordia line with an upper concordia intercept age of 1793 \pm 7 Ma (Fig. 6g), which is identical, within error, to the $^{207}\text{Pb/}^{206}\text{Pb}$ weighted average age of 1791 \pm 8 Ma (Fig. 6h) obtained from twenty concordant analyses. The $^{207}\text{Pb/}^{206}\text{Pb}$ weighted average age of 1791 \pm 8 Ma is interpreted as the emplacement age for this granite. Additionally, eight analyses form a single population and yield a $^{207}\text{Pb/}^{206}\text{Pb}$ weighted average age of 1870 \pm 13 Ma (Table 1), interpreted as inherited zircon grains.

4.3. Wonga-Burstall Igneous Event (1750-1690 Ma)

4.3.1. Sample SP01, SP22 and SP24- Steeles Granite

The Steeles Granite intrudes the Sulieman Gneiss and the Alpha Centaury Metamorphics. The eastern side is in structural contact with the Jayah Creek Metabasalt whereas on the western side is cut by the Rufus Fault. In the northern part, the Steeles Granite intrudes into a gneissic granite unit mapped as Sybella Granite. The Steeles Granite was previously assigned to the Sybella Igneous Event, but our results indicate it belongs to the Wonga-Burstall Igneous Event.

Samples SP01 and SP22 were collected from the main phase of the Steeles Granite along the Boulia–Mount Isa Highway and consist of porphyritic biotite granite (Fig. 3c). The Steeles Granite is mainly coarse grained, porphyritic, with large (up to 4 cm) potassic feldspar crystals in a matrix of coarse quartz and biotite. Dykes and smaller intrusions are common within the Steeles Granite, and they consist of leucocratic biotite granite, leucogranite, biotite-hornblende granodiorite, microgranite and pegmatites. Xenoliths of various igneous compositions are common within the Steeles Granite. Dolerite dykes of variable thickness crosscut the granite. The central part of the granite is weakly deformed; the deformation intensity increases towards the margins and may contain localized zones of intense deformation. The foliation trends northwest southeast and is subvertical. Sample SP01 was collected from a weakly deformed granite (Fig. 4h) whereas sample SP22 was collected from a well foliated granite (Fig. 4i).

Sample SP01 yielded zircons that are mainly euhedral and prismatic with a small number of grains having a subhedral morphology and they are brown to colourless. CL images reveal the presence of growth zoning with low luminescence zone in the cores and higher luminescence zones towards the rims. Twenty-one zircon grains define a discordia line with an upper concordia intercept age of 1686 \pm 6 Ma (Fig. 7a) which is similar, within uncertainty, to the $^{207}\text{Pb}/^{206}\text{Pb}$ weighted average at 1693 \pm 9 Ma (Fig. 7b) obtained from seventeen concordant grains. The 1693 \pm 9 Ma $^{207}\text{Pb}/^{206}\text{Pb}$ weighted average age is considered to represent the magmatic crystallization age for this granite.

Sample SP22 yielded prismatic zircon grains that are euhedral to subhedral shaped and brown to colourless under the binocular microscope. CL images reveal the presence of weakly zoned and homogenous zircon grains with overall low luminescence except a few grains that display a higher luminescence towards the rims. Nineteen zircons define a discordia line with an upper intercept age of 1705 ± 7 Ma (Fig. 7c), which is identical, within uncertainty, to the $^{207}\text{Pb}/^{206}\text{Pb}$ weighted average age of 1697 ± 6 Ma (Fig. 7d) obtained from fifteen concordant grains. The 1697 ± 6 Ma $^{207}\text{Pb}/^{206}\text{Pb}$ weighted average age is considered the magmatic crystallization age of this sample. Additionally, eleven concordant grains yielded a $^{207}\text{Pb}/^{206}\text{Pb}$ weighted average age of 1744 ± 9 Ma. These grains are interpreted as inherited (Table 1).

In the central part of the Steeles Granite occurs a series of small, compositionally distinct, northwest trending granitic intrusions crosscut

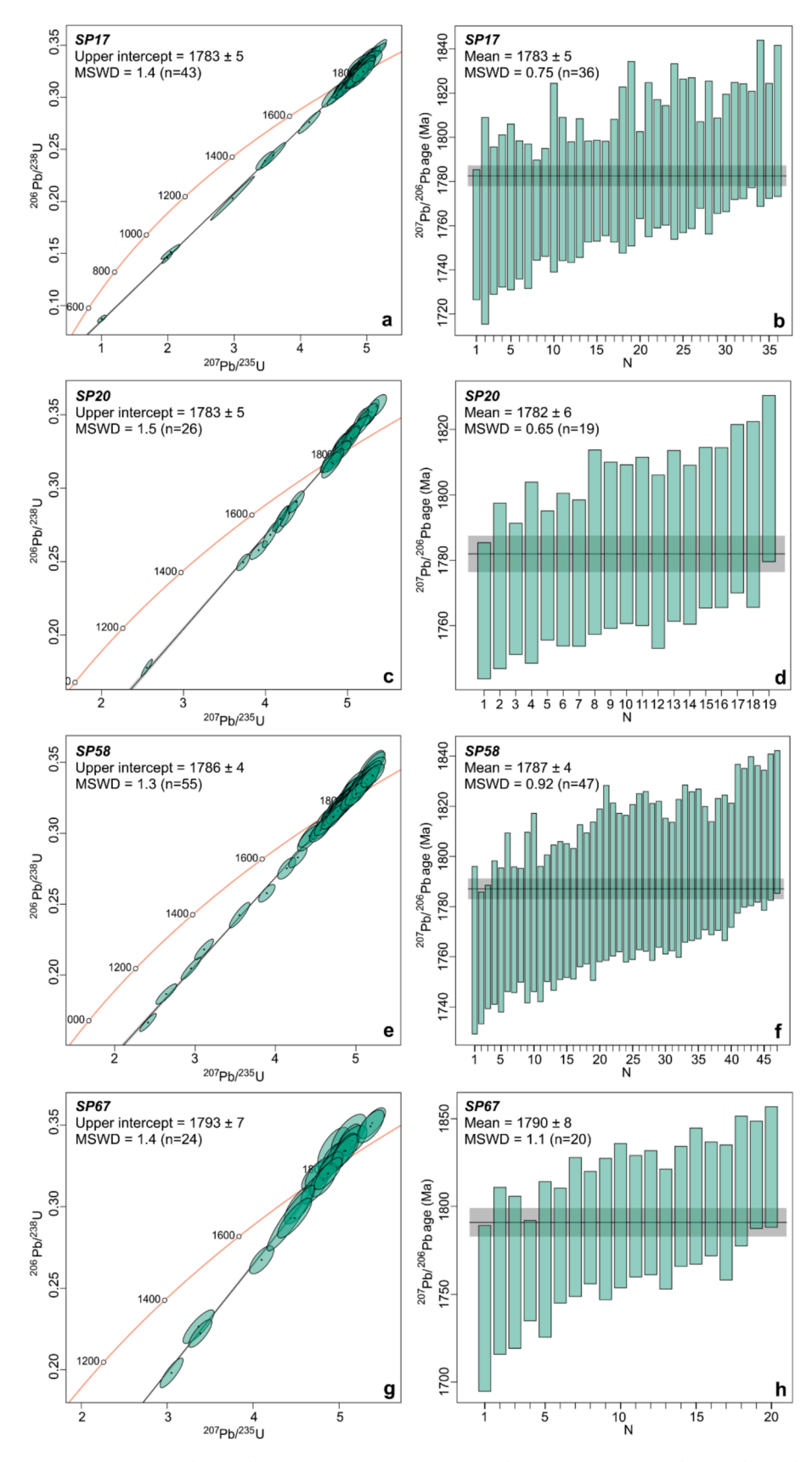


Fig. 6. U-Pb zircon data from magmatic zircons of the Argylla Igneous Event consisting of samples SP17, SP20, SP58 and SP67. The results are illustrated as an upper intercept age on concordia plots and as weighted averages.

Table 1Summary of ²⁰⁷Pb/²⁰⁶Pb ages (weighted average) from the intrusive rocks sampled from the Dajarra region. Coordinates are GDA94 UTM.

Previous interpretation	New defining of this study	Intrusive name	Sample	Easting	Northing	Age (Ma)	Age comment	Inherited zircons [n; MSWD]
Kalkadoon Igneous Event (1870–1840 Ma)	Kalkadoon Igneous Event	Kalkadoon Granodiorite	SP19	351,484	7,595,987	1856 ±	n = 22 MSWD = 1.4	
		Sulieman Gneiss	SP36	324,082	7,602,967	1854 ± 6	n = 16 MSWD = 1.6	
Wonga-Burstall Igneous Event (1750–1690 Ma)	Argylla Igneous Event	Camel Creek Granite	SP16	354,072	7,606,668	1801 ± 12	n = 8 MSWD = 1.7	
		Camel Creek Granite	SP33	353,941	7,606,676	1784 ± 3	n = 86 MSWD = 0.79	
		Garden Creek Porphyry	SP17	350,710	7,606,745	1783 ± 5	n = 36 MSWD = 0.75	$1827 \pm 10 \; [11; 0.66]$
Sybella Igneous Event (1680–1650 Ma)		Unnamed granite	SP20	323,250	7,602,768	1782 ± 6	n = 19 MSWD = 0.65	$1823 \pm 9 \ [9; 0.1], 1869 \pm \\ 13 \ [5; 0.98]$
		Unnamed granite	SP67	324,234	7,590,364	1791 ± 8	n = 16 MSWD = 0.8	$1870 \pm 13 \; [8; 0.54]$
		Unnamed granite	SP58	311,441	7,562,176	1787 ± 4	n = 47 MSWD = 0.92	$1829 \pm 9 \; [11; 1.1]$
	Wonga-Burstall Igneous Event	Steeles Granite	SP01	327,616	7,602,354	1693 ± 9	n = 17 MSWD = 0.87	
		Steeles Granite	SP22	326,518	7,602,768	1697 ± 6	n = 15 MSWD = 0.95	$1744 \pm 9 \; [11; 0.5]$
		Unnamed granite	SP24	325,625	7,601,793	1704 ± 9	n = 17 MSWD = 1	$1775 \pm 9 \ [15; 1.6], 1873 \\ \pm 19 \ [6; 1.3]$
		Unnamed granite	SP65	318,657	7,565,571	1713 ± 10	n = 11 MSWD = 0.45	$1770 \pm 22 \ [2; 0.04]$
		Copper Valley Granite	SP61	317,780	7,564,568	1695 ± 8	n = 7 MSWD = 1.5	1742 ± 11 [4; 0.6]
	Sybella Igneous Event	Unnamed granite	SP47	316,976	7,567,736	1665 ± 14	n = 8 MSWD = 1.8	

by a dolerite dyke. Sample SP24 was collected from one of these intrusions (Fig. 3c). These intrusions are granodioritic in composition, coarse grained, phaneritic and consist of quartz, feldspar, biotite and hornblende (Fig. 4j). They contain xenoliths of various igneous phases including porphyritic biotite granite and locally along the margins a transitional zone to the main phase of the Steels Granite can be found.

Zircon grains from sample SP24 are colourless and semi-translucent, have elongate to prismatic shapes and subhedral morphologies. Growth zoning with low luminescence cores surrounded by higher luminescence rims is common in the CL images. Eighty zircons from this sample yield concordant ages with thirty-eight analyses. Seventeen concordant grains define a discordia line with an upper intercept age of 1709 \pm 17 Ma (Fig. 7e), which is identical, within uncertainty, to the $^{207}\text{Pb}/^{206}\text{Pb}$ weighted average age of 1705 \pm 9 Ma (Fig. 7f) obtained from the same analyses. The 1705 \pm 9 Ma $^{207}\text{Pb}/^{206}\text{Pb}$ age is interpreted as the emplacement age for this granite. Twenty-one zircon grains with concordant analyses yielded older ages. Fifteen of these grains form a single population with a $^{207}\text{Pb}/^{206}\text{Pb}$ weighted average ages of 1775 ± 9 Ma (Table 1) whereas the remining six grains form a single population with a $^{207}\text{Pb}/^{206}\text{Pb}$ weighted average ages of 1873 \pm 19 Ma (Table 1). These two older populations are interpreted to represent inherited zircon grains.

4.3.2. Sample SP61 - Copper Valley Granite

Sample SP61 was collected from an intrusive unit located in the southwestern part of the Dajarra region and mapped as the Copper

Valley Granite (Fig. 3e). The intrusion consists of two different plutons intruding into the Sulieman Gneiss and the Alpha Centauri Metamorphics. The granite is fine to medium grained, equigranular, composed mainly of quartz, feldspar, biotite and muscovite that underwent intense deformation and metamorphism with migmatites developed locally (Fig. 4k). The Copper Valley Granite was mapped on geological maps as belonging to the Sybella Igneous Event but our dating suggests it belongs to the Wonga-Burstall Igneous Event.

Zircon grains from sample SP61 are brown to colourless and have subhedral to subrounded shapes. Metamictization and low to moderate luminescence were observed from CL images. Sixteen zircon grains define a discordia line with an upper concordia intercept age of 1694 ± 9 Ma (Fig. 7g), which is identical, within uncertainty, to the $^{207}\text{Pb}/^{206}\text{Pb}$ weighted average age at 1695 ± 8 Ma (Fig. 7h) obtained from eight concordant grains and interpreted as the magmatic crystallization age for the Copper Valley Granite. Additionally, there are four concordant grains that define a single population with $^{207}\text{Pb}/^{206}\text{Pb}$ weighted average age of 1742 ± 11 Ma interpreted as inherited grains (Table 1).

4.3.3. Sample SP65 – Unnamed Granite

Sample SP65 was collected from a granite dyke trending NNE–SSW that intruded into the basement rocks of the Sulieman Gneiss (Fig. 3e and Fig. 4l). This dyke occurs close to the Copper Valley Granite and is most likely part of the same intrusive event which was previously assigned to the Sybella Igneous Event but our dating suggests it belongs to the Wonga-Burstall Igneous Event.

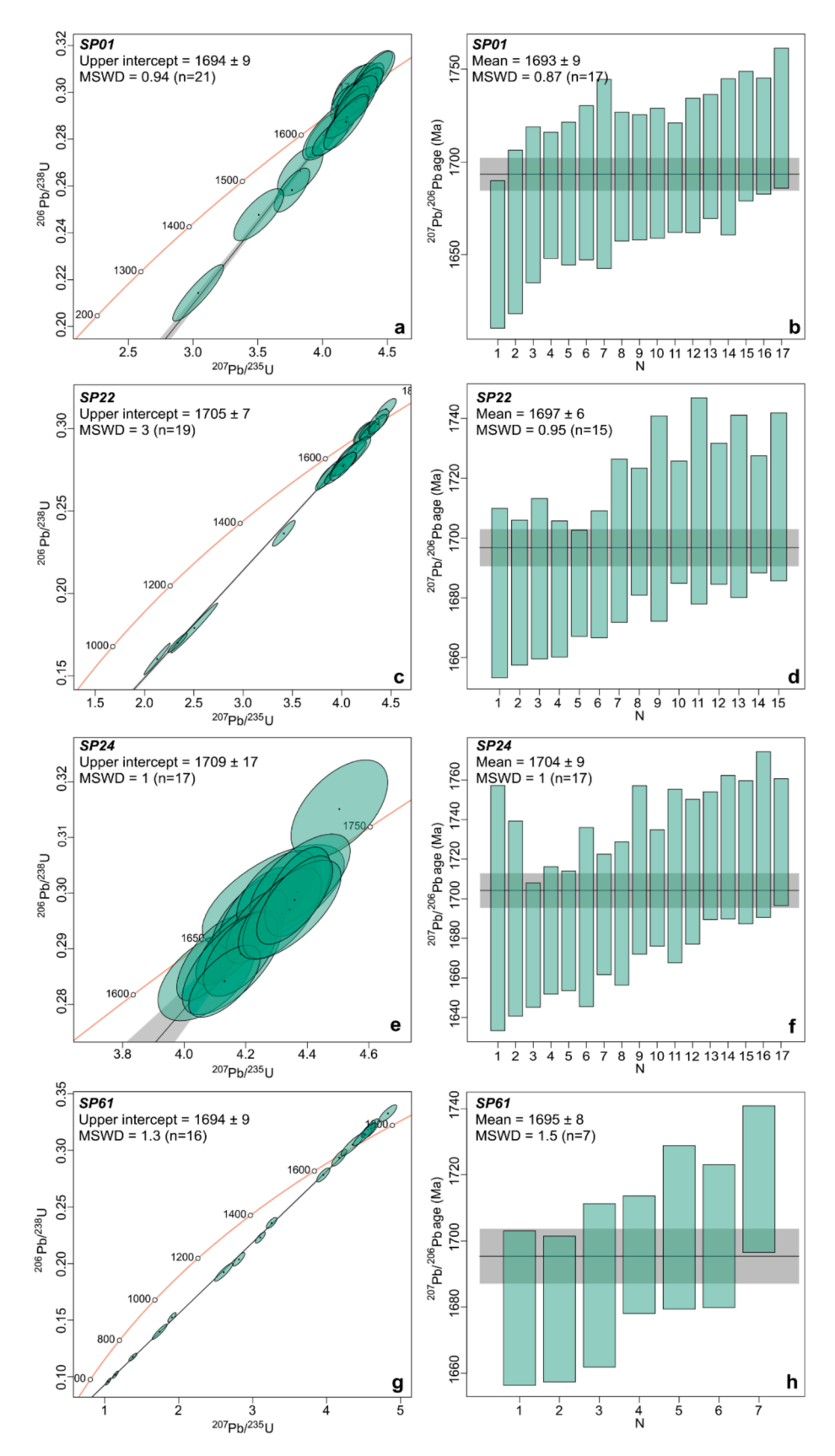


Fig. 7. U-Pb zircon data from magmatic zircons of the Wonga-Burstall Igneous Event including samples SP01, SP22, SP24 and SP61. The results are shown as an upper intercept age on concordia plots and as weighted averages.

Zircon grains separated from sample SP65 are colourless, prismatic and subhedral to euhedral shaped. The CL mages reveal growth zoning with low to moderate luminescence and metamictization. Twenty-three analyses define a discordia line with an upper concordia intercept age of 1713 ± 10 Ma (Fig. 8a), which is identical to the $^{207}\text{Pb}/^{206}\text{Pb}$ weighted average age of 1713 ± 10 Ma (Fig. 8b) obtained from eleven concordant grains. The $^{207}\text{Pb}/^{206}\text{Pb}$ weighted average age of 1713 ± 10 Ma is interpreted to represent the emplacement age of this granite dyke. Moreover, there are two inherited grains that yield a combined $^{207}\text{Pb}/^{206}\text{Pb}$ weight average age of 1770 ± 22 Ma (Table 1).

4.4. Sybella Igneous Event (1680-1650 Ma)

4.4.1. Sample SP47 - Sybella Granite

Sample SP47 has been mapped as Sybella Granite and assigned as the Sybella Igneous Event. This sample was collected from a pluton located in the southwestern part of the Dajarra region (Fig. 3e). The pluton intrudes into the Alpha Centaury Metamorphics and the Jayah Creek Metabasalt whereas its northern part is cut by the Rufus Fault. It is foliated, medium to coarse grained porphyritic granite composed mainly of quartz, feldspar and biotite (Fig. 4f).

Zircons grains from sample SP47 are dominated by subhedral shaped grains varying from colourless to translucent under the binocular

microscope. They are low to moderate luminescence with weakly defined concentric growth zoning. Twenty-two analyses define a discordia line with an upper concordia intercept age of 1667 \pm 12 Ma (Fig. 8c), which is identical, within uncertainty, to the $^{207}\text{Pb}/^{206}\text{Pb}$ weighted average age at 1665 \pm 14 Ma (Fig. 8d) obtained from eight concordant grains. The 1665 \pm 14 Ma $^{207}\text{Pb}/^{206}\text{Pb}$ weighted average age is interpreted as representative of the magmatic crystallization age for this sample.

4.5. Zircon Lu-Hf isotopic data

Zircon Hf isotopic analyses were conducted on 70 zircon grains from thirteen samples representing newly constrained intrusive events in the Dajarra region. These results are presented as initial $^{176} \mathrm{Hf}/^{177} \mathrm{Hf}$ ratios and $\epsilon \mathrm{Hf}_{(t)}$ values plotted against interpreted crystallization ages (Figs. 9a and b). Zircon grains separated from the Kalkadoon Granodiorite and the Sulieman Gneiss, with crystallization ages at ca. 1850 Ma, have similar Hf isotopic composition and yield initial $^{176} \mathrm{Hf}/^{177} \mathrm{Hf}$ ratios ranging from 0.281446 to 0.281603, and have $\epsilon \mathrm{Hf}_{(t)}$ values between 0.0 and -5.5.

Zircon grains separated from intrusive units with ages between ca. 1810 and 1780 Ma have unradiogenic Hf isotopic composition except SP58 which is the only sample with radiogenic composition. The two

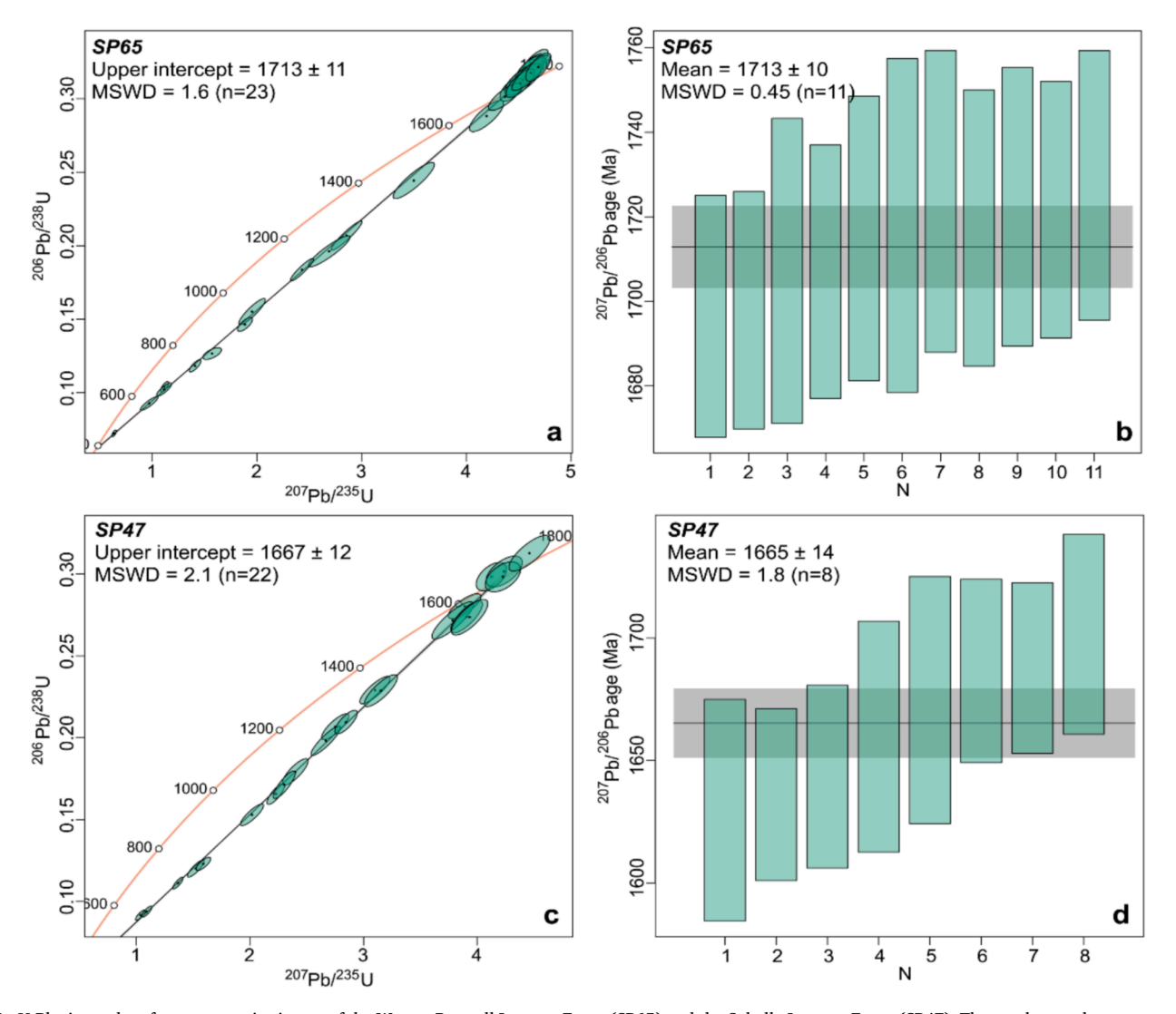


Fig. 8. U-Pb zircon data from magmatic zircons of the Wonga-Burstall Igneous Event (SP65) and the Sybella Igneous Event (SP47). The results are shown as an upper intercepted age on concordia plots and as weighted averages.

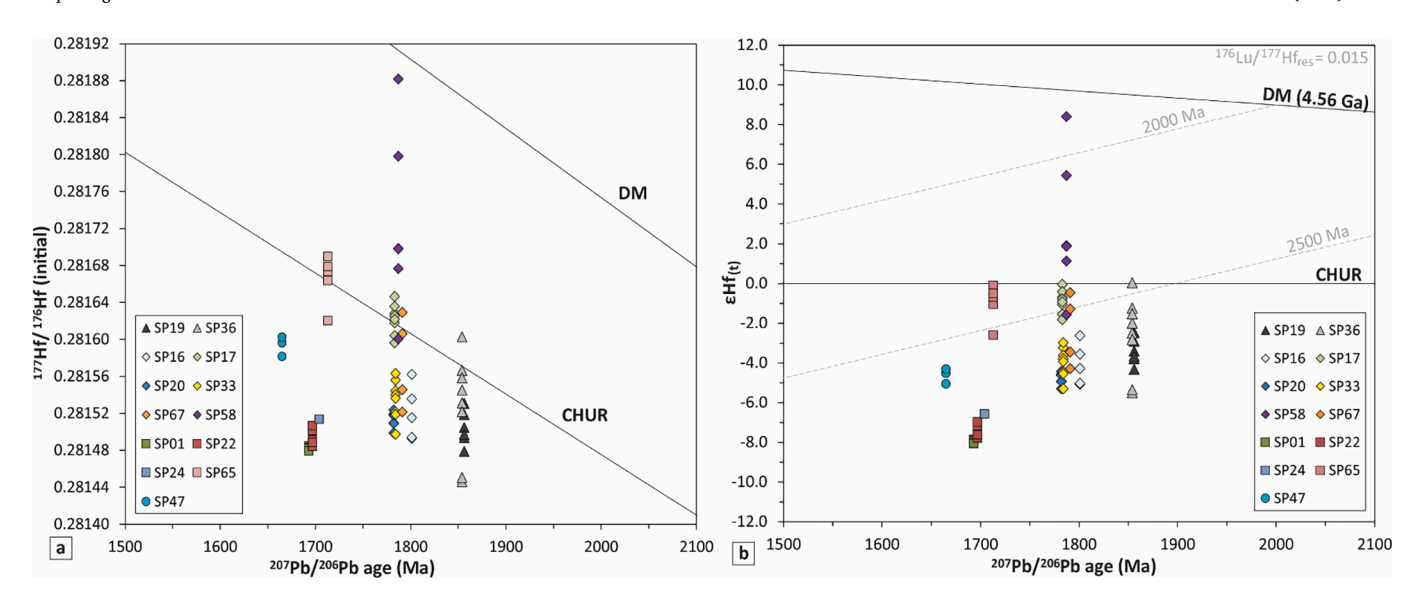


Fig. 9. Hf isotopic data for magmatic zircons from the Dajarra region. No Hf isotropic data were collected on sample SP61 due to small grain sizes. Diagrams illustrate the initial 176 Hf ratios (a) and ε Hf_(t) values (b) plotted against interpreted crystallization ages. 176 Lu/ 177 Hf ref = 0.015 (ε Hf Ma $^{-1}$ = 0.012) regarding to evolution lines of Proterozoic shales (Spencer et al., 2020; Vervoort & Blichert-Toft, 1999). CHUR = chondritic uniform reservoir. DM = depleted mantle.

samples collected from the Camel Creek Granite (SP16, SP33) have similar Hf isotopic compositions with the ¹⁷⁶Hf/¹⁷⁷Hf ratios varying between 0.281493 and 0.281563 whereas the $\varepsilon Hf_{(t)}$ values vary between -2.6 and -5.3. Zircon grains analysed from sample SP20 show very little variation in the Hf isotopic composition with the 176 Hf/ 177 Hf ratios varying between 0.281499 and 0.281524 whereas the $\varepsilon Hf_{(t)}$ values vary between -4.4 and -5.3. The 176 Hf/ 177 Hf ratios of zircons form sample SP67 vary between 0.281522 and 0.281629 whereas the $\varepsilon Hf_{(t)}$ values vary between -0.5 and -4.3. Zircon grains analysed from the Garden Creek Porphyry (SP17) also shows little variation with the ¹⁷⁶Hf/¹⁷⁷Hf ratios varying between 0.281596 and 0.281646 whereas the εHf(t) values vary between + 0.0 and -1.8. One unnamed granite (SP58 with a $^{207}\text{Pb}/^{206}\text{Pb}$ weighted average age of 1787 \pm 4 Ma), located in the southwestern corner of the Dajarra region and intruding into the Oroopo Metabasalt, plots above the CHUR line, indicating a more radiogenic signature. The ¹⁷⁶Hf/¹⁷⁷Hf ratio of zircon grains from this sample varies between 0.281601 and 0.281882 whereas the EHf(t) values vary between + 8.4 and -1.6.

Zircon grains from intrusive units with ages between ca. 1710 and 1690 Ma have unradiogenic Hf isotopic compositions. The two samples from the Steeles Granite (SP01 and SP22) have very similar zircon Hf isotopic compositions with the $^{176}\mathrm{Hf}/^{177}\mathrm{Hf}$ ratio varying between 0.281479 and 0.281507 whereas the $\epsilon\mathrm{Hf}_{(t)}$ values vary between -7.0 and -8.1. Due to the small grain size only one zircon grain from sample SP24 was analysed for Hf isotopic composition with a $^{176}\mathrm{Hf}/^{177}\mathrm{Hf}$ ratio of 0.281514 and an $\epsilon\mathrm{Hf}_{(t)}$ value of -6.6. Zircon grains from sample SP65 have a $^{176}\mathrm{Hf}/^{177}\mathrm{Hf}$ ratio that varies between 0.28162 and 0.28169 whereas the $\epsilon\mathrm{Hf}_{(t)}$ values vary between -0.1 and -2.6.

Sample SP47 with an emplacement age of 1665 ± 14 Ma has zircon grains with $^{176}\text{Hf}/^{177}\text{Hf}$ ratios between 0.281582 and 0.281602 and $\epsilon\text{Hf}_{(t)}$ values between -4.3 and -5.1.

5. Discussion

5.1. Implications for the stratigraphy and stratigraphic correlations

The field relationships and the emplacement ages for the Kalkadoon Granite, the Camel Creek Granite and the Garden Creek Porphyry have implications for the stratigraphic relationships and correlations in the Mount Isa Inlier, particularly for the Bottletree Formation and the Mount Guide Formation. The Bottletree Formation, dated at ca. 1790 Ma (Page,

1983) is typically interpreted to uncomfortably overlie the Kalkadoon Granodiorite and other rocks of the Kalkadoon Leichhardt Belt, to form the base of the Leichhardt Superbasin and as the Western Succession equivalent of the Argylla Formation (Derrick et al., 1977; Foster & Austin, 2008; Neumann et al., 2006; Spampinato et al., 2015). However, the map pattern and our field observations suggest that the Kalkadoon Granite, dated at 1856 \pm 6 Ma, intrudes the Bottletree Formation in the Dajarra area (Fig. 3b). Moreover, the Camel Creek Granite, dated between ca. 1800 and 1780 Ma, clearly intrudes the Bottletree Formation and contains enclaves of the surrounding country rock (Fig. 3b). These relationships demonstrate that at least in the Dajarra area the Bottletree Formation is much older or that these rock units do not belong to the Bottletree Formation and need to be reassigned. Initially, Derrick et al. (1977) proposed that the Bottletree Formation is the Western Succession equivalent of the Argylla Formation whereas Blake (1980) proposed that the formation is much older and has no stratigraphic equivalent in the Eastern Succession. The current stratigraphic position of the Bottletree Formation is based on two zircon age dates from the northern part of the sequence at ca. 1808 and 1790 Ma (Page, 1983). The two dated samples are described as porphyritic metadacites undisturbed by the regional deformation and metamorphism (Page, 1983). It is possible that they represent intrusive dykes rather than volcanic flows, postdate the deposition of the formation and the two zircon ages are unrelated to the timing of deposition of the Bottletree Formation. While this is speculative in the absence of direct field observations, in conjunction with the new field observations and ages for the Kalkadoon Granite and the Camel Creek Granite, it is clear that the issue regarding the stratigraphic position and continuity of the Bottletree Formation remains unresolved. Our interpretation is consistent with the observations of Blake (1980) and indicate that the Bottletree Formation is older than the Argylla Formation and has no Eastern Succession equivalent.

The Garden Creek Porphyry trends north–south and intrudes the Mount Guide Quartzite over a length of ~40 km despite being only $\sim100\text{--}200$ m wide and very likely represents a vertical intrusion (Fig. 3b). The Mount Guide Quartzite on the other hand is internally tightly folded along north–south axes, the layering dips both east and west at angles varying between 20° and 85° and overturned bedding is common, especially along the eastern margin of the formation. All these observations suggest that not only the intrusion of the Graden Creek Porphyry postdates the deposition of the Mount Guide Quartzite, but it also postdates most of the deformation that affected these rocks. Maximum

depositional ages for Mount Guide Quartzite from the northern part of the Western Succession, near Mount Isa town, are ca. 1793 Ma for the lower part and ca. 1773 Ma for the upper part of the formation (Neumann et al., 2006). The new emplacement age for the Garden Creek Porphyry at 1783 \pm 5 Ma indicates that in the southern part of the inlier the units mapped as the Mount Guide Quartzite are either older or are not stratigraphic equivalents to the units mapped as Mount Guide Quartzite in the northern part. Based on the observations that the units mapped as Mount Guide Quartzite in the Dajara area were deformed and metamorphosed prior to the intrusion of the Garden Creek Porphyry we suggest that these units should be assigned a different name and their stratigraphic position be reassessed.

5.2. Inlier wide magmatic activity

The compilation of U-Pb zircon ages suggests that the magmatic history of the Mount Isa Inlier can be separated into six igneous events (Fig. 2). The Kalkadoon Igneous Event (ca. 1880-1850 Ma) is a welldefined period of igneous activity in the Mount Isa Inlier (Bultitude et al., 2021; Page, 1978; Withnall, 2019) but until this study all igneous rocks of this age were known only from the Kalkadoon-Leichhardt Belt and from the Mary Katheleen Domain (Bierlein et al., 2008; Bultitude et al., 2021). We have shown that the Sulieman Gneiss, from the Western Succession also belongs to this igneous event and probably other units mapped as Pre-Barramundi basement (i.e. Saint Ronan Metamorphics), are similar in age. The units mapped as Pre-Barramundi basement (Fig. 3a) occur along the western margin of the exposed Precambrian rocks forming a north-south trending zone, sub-parallel to the Kalkadoon-Leichhardt Belt whereas the intervening rocks are younger. We propose that the units mapped as Pre-Barramundi basement and the units forming the Kalkadoon-Leichhardt Belt are equivalent and prior to ca. 1820 Ma they formed a continuous unit along the eastern margin of the North Australia Craton. The Kalkadoon Granite and the Sulieman Gneiss have an almost identical Hf isotopic signature (Fig. 9) not only with each other but also with similar age rocks from the Kalkadoon-Leichhardt Belt (Fig. 10) suggesting at least similarity in source material if not a common genesis.

Our data suggests that there are numerous intrusive rocks in the Dajarra region with emplacement ages between ca. 1800 and 1780 Ma (Table 1; Fig. 3a) belonging to the ca. 1820–1770 Ma Argylla Igneous Event. Previously, these intrusive rocks were assigned to either the Wonga-Burstall Igneous Event (Camel Creek Granite, Garden Creek Porphyry) or the Sybella Igneous Event (unnamed granites, samples SP20, SP67 and SP58). Until recently, in Mount Isa Inlier, the only felsic intrusive rocks with ages between ca. 1820 and 1770 Ma were known from the Big Toby and Yeldham granites (Carson et al., 2011; Wyborn et al., 1988) from the Western Succession but recent work (Cocker et al., 2025; Le et al., 2021a) found numerous granitic intrusions within this age bracket from the Mary Kathleen Domain and from deep drill core sample (Olierook et al., 2022) south of the Dajarra region. The Argylla Formation (felsic volcanics, volcaniclastics and metasediments), from the Eastern Succession has similar ages suggesting that the plutonic activity ranging from ca. 1820-1770 Ma has an extrusive equivalent. Similar, to other intrusive events from the Mount Isa Inlier, the Argylla Igneous Event forms two north-south trending subparallel belts, one located in the Eastern Succession, and one located in the Western Succession (Fig. 2a). The Hf isotopic composition of zircon grains from these igneous rocks is mostly unradiogenic with negative $\varepsilon Hf_{(t)}$ values suggesting derivation from reworked crustal material, except for the sample SP58 that is dominated by radiogenic Hf and positive $\varepsilon Hf_{(t)}$ values consistent with derivation from a more primitive source (Fig. 9). Considering that the Argylla Igneous Event is synchronous with the emplacement of the mafic Eastern Creek Volcanics and the equivalent Jayah Creek Metabasalt, it is surprising that only one granitic intrusion

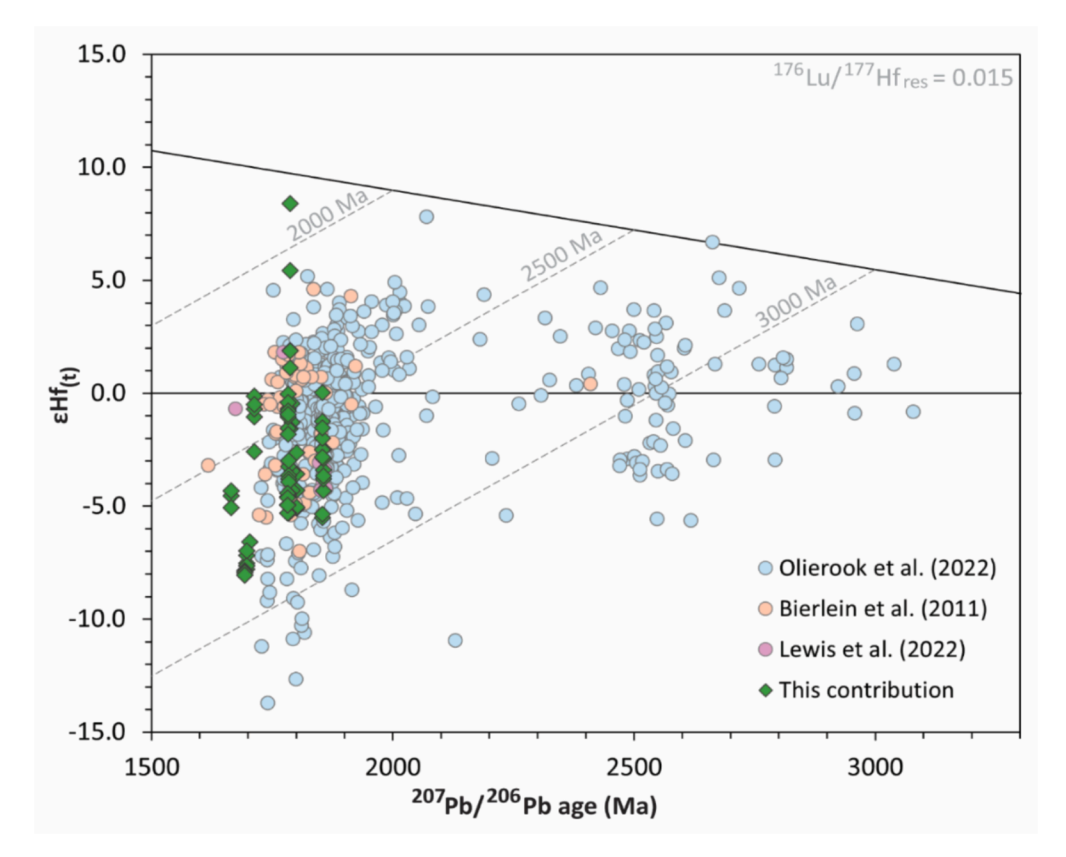


Fig. 10. Hf isotopic data for magmatic zircons from the Dajarra region plotted against a compilation of Hf isotope data from Mount Isa Inlier (Bierlein et al., 2011; Lewis et al., 2022; Olierook et al., 2022). 176 Lu/ 177 Hf $_{ref} = 0.015$ (ϵ Hf Ma $^{-1} = 0.012$) regarding to evolution lines of Proterozoic shales (Spencer et al., 2020; Vervoort & Blichert-Toft, 1999). CHUR = chondritic uniform reservoir. DM = depleted mantle.

indicates derivation from a mantle source. The overall Hf isotopic composition (Fig. 10) of igneous rocks emplaced during the Argylla Igneous Event is also dominated by unradiogenic Hf and negative $\epsilon Hf_{(t)}$ values suggesting that the mantle event that resulted in the emplacement of Eastern Creek Volcanics and equivalent mafic rocks was also responsible for intracrustal melting and the generation of crustal melts across the inlier.

The Dajarra area also contains intrusive rocks belonging to the Wonga-Burstall Igneous Event such as the Steeles Granite, the Copper Valley Granite and unnamed intrusion (SP65). In general, igneous rocks belonging to the Wonga-Burstall Igneous Event are mainly found in the Eastern Succession, particularly in the Mary Kathleen Domain and were emplaced during the ca. 1750 to 1710 Ma Wonga Orogeny (Spence et al., 2021, 2022) with most intrusions having emplacement ages between ca. 1740 and 1720 Ma. Prior to this study the only intrusive rocks with similar ages from the Western Succession was the Weberra Granite, in the far northern part of the inlier, with emplacement ages at ca. 1711-1698 Ma (Neumann et al., 2006; Wyborn et al., 1988). The new granite ages from the Dajarra region span the same time interval, ca. 1711 to 1693 Ma, with the Weberra Granite indicating that the Wonga-Burstall Igneous Event in the Western Succession postdates the emplacement of the Wonga-Burstall plutons in the Eastern Succession. The ca. 1710 to 1690 Ma magmatism from the Western Succession could represent the waning states of the Wonga Orogeny as well as indicate a migration of magmatic activity towards west. The Hf isotopic composition of the ca. 1710 to 1690 Ma intrusions (Fig. 9) is dominated by unradiogenic Hf with negative $\varepsilon Hf_{(t)}$ values consistent with the Hf isotopic composition of similar aged granites (Fig. 10) from other parts of the inlier and indicate magma derivation primarily by crustal reworking.

The last igneous event recognised in the Dajarra area is the Sybella Igneous Event although only one intrusion from the southwestern corner (SP47; Fig. 3e) has emplacement ages at 1665 ± 14 Ma consistent with this igneous event. Prior to this study most of the intrusions in this region were assigned to the Sybella Igneous Event but it is clear now that the magmatic activity associated with the emplacement of the Sybella batholith is restricted to the area west of the Rufus Fault and with the exception of the unnamed granite dated in this study at 1665 ± 14 Ma there are no granites of this age east of the Rufus fault. Magmatism of this age is rare in the Eastern Succession, and the bulk of magmatic activity appears to have occurred in the Western Succession. There is limited zircon Hf isotopic composition available for rocks belonging to the Sybella Igneous Event, but the rocks analysed in this study appear to be dominated by unradiogenic Hf with negative ϵ Hf_(t) values consistent with derivation from reworking crustal material (Fig. 9).

5.3. Tectonic and geodynamic setting along the eastern margin of the north Australia Craton (NAC)

5.3.1. The 1880–1850 Ma Kalkadoon Igneous Event and the Barramundi Orogeny

The Barramundi Orogeny, a widespread orogenic event in the NAC, occurred between ca. 1890 and 1850 Ma and affected the entire eastern margin of the NAC (e.g. Bierlein et al., 2011; Etheridge et al., 1987; Gibson et al., 2025). It is typically interpreted as a Cordilleran style orogeny build on older continental crust (Gibson et al., 2025). However, in the Mount Isa Inlier the oldest known rocks belong to the Kalkadoon Igneous Event, and so far, no rocks predating this igneous event have been found in the inlier. Rocks mapped as Pre-Barramundi basement such as the Yarringa Metamorphics, the Kurbayia Metamorphic Complex, Saint Ronan Metamorphics, Sulieman Gneiss and the Plum Mountain Gneiss consistently return U-Pb zircon ages within the ca. 1890 to 1850 Ma interval thus overlapping with the Kalkadoon Igneous Event (Bultitude et al., 2021; Cocker et al., 2025; Withnall, 2019). The Kalkadoon Igneous Event is generally considered to have occurred during the final stages of the Barramundi Orogeny (e.g. Bierlein et al.,

2011; Neumann et al., 2009; Page & Williams, 1988), however, in the light of the data presented here and the lack of older rocks we consider that it actually represents the defining geological activity for the Barramundi Orogeny in the Mount Isa Inlier and should be seen as a series of magmatic events occurring during the entire orogenic cycle. The only indication of older basement comes from inherited zircons and from Hf (Fig. 10) and Nd isotopic compositions which are consistent with reworking of older (>2Ga) crust during the Barramundi Orogeny (e.g. Bierlein et al., 2011; Wyborn et al., 1992). The lack of primitive magmas and older rocks is puzzling and suggest that whatever the tectonic environment during the Barramundi Orogeny was somehow different from modern Cordilleran style orogeny. Similar age igneous rocks, the Donington Suite, are found in the SAC and in some tectonic reconstructions (Reid et al., 2008a), the Kalkadoon-Leichhardt Belt and the Donington Suite are interpreted to form a continuous belt since the Barramundi Orogeny (Fig. 11a; Gibson et al., 2025). If the Mount Isa Inlier and fragments of the SAC were linked since the Barramundi Orogeny it could explain the presence of Archean detrital zircons in Mount Isa Inlier by sourcing them from the Gawler Craton without the need of a proximal Archean source rocks.

5.3.2. The 1820–1770 Ma Argylla Igneous Event – Rifting or collisional magmatism?

The Argylla Igneous Event is synchronous with similar aged magmatic events from the NAC such as the ones in the Arunta Inlier, the Granites Tanami and the Halls Creek orogens (e.g. Bagas et al., 2010; Claoué-Long & Edgoose, 2008; Crispe et al., 2007; Hand and Buick, 2001; Howlett et al., 2015; Iaccheri, 2019; Page et al., 2001). However, there are certain discrepancies in the tectonic interpretations between these terrains and the Mount Isa Inlier during this period. The emplacement of granites in the ca. 1820 to 1770 Ma interval in the Arunta Inlier, the Granites Tanami and the Halls Creek orogens are attributed to orogenic events and collisional tectonics related to the final assembly of the Nuna supercontinent (e.g. Betts et al., 2016; Gibson et al., 2025) whereas in the Mount Isa Inlier this period is in general interpreted to represent intracontinental rifting associated with the opening of the Leichhardt Superbasin (Derrick, 1982; O'Dea et al., 1997a; O'Dea et al., 1997b; Passchier & Williams, 1989). The main arguments favouring this tectonic scenario in Mount Isa Inlier relies on the presence of extensive bimodal volcanism represented by mafic volcanism of the Eastern Creek Volcanics and felsic volcanism of the Bottletree Formation in the Western Succession and by the mafic Magna Lynn Metabasalt and the felsic volcanic rocks of the Argylla Formation in the Eastern Succession. Moreover, these units occur as continuous, linear, north-south trending belts along the lengths of the inlier interpreted to indicate east-west rifting on either side of the Kalkadoon-Leichhardt Belt either due to plume activity (O'Dea et al., 1997b) or because of back-arc extension and rifting behind a distal arc in the Arunta Inlier (Fig. 11b; Giles et al., 2002; Scott et al., 2000). The presence of extensive intrusive magmatism during this period brings some new perspectives to the tectonic interpretation and the geodynamic setting of Mount Isa Inlier. Firstly, as discussed above, the continuity and timing of some stratigraphic units (Bottletree Formation, Mount Guide Quartzite) in the southern part of the inlier needs revising. This can have crucial implications for the tectonic interpretation. For example, if the units mapped as Mount Guide Quartzite in the southern part of the inlier do not belong to the Haslingden Group, it is also possible that the stratigraphic units overlying the Mount Guide Quartzite such as the Eastern Creek Volcanics and the Jayah Creek Metabasalt from this part of the inlier are also older. If this is the case, the volume and spatial extend of the Easter Creek Volcanics will be significantly reduced and the geometry and extent of the interpreted rift will have to be reassessed. Secondly, recent results from the Tick Hill area (east of Dajarra) documented ca. 1800 to 1770 Ma magmatism that intruded during compressional deformation and the formation of upright tight fold at upper amphibolite facies conditions (Le et al., 2024). In the Dajarra

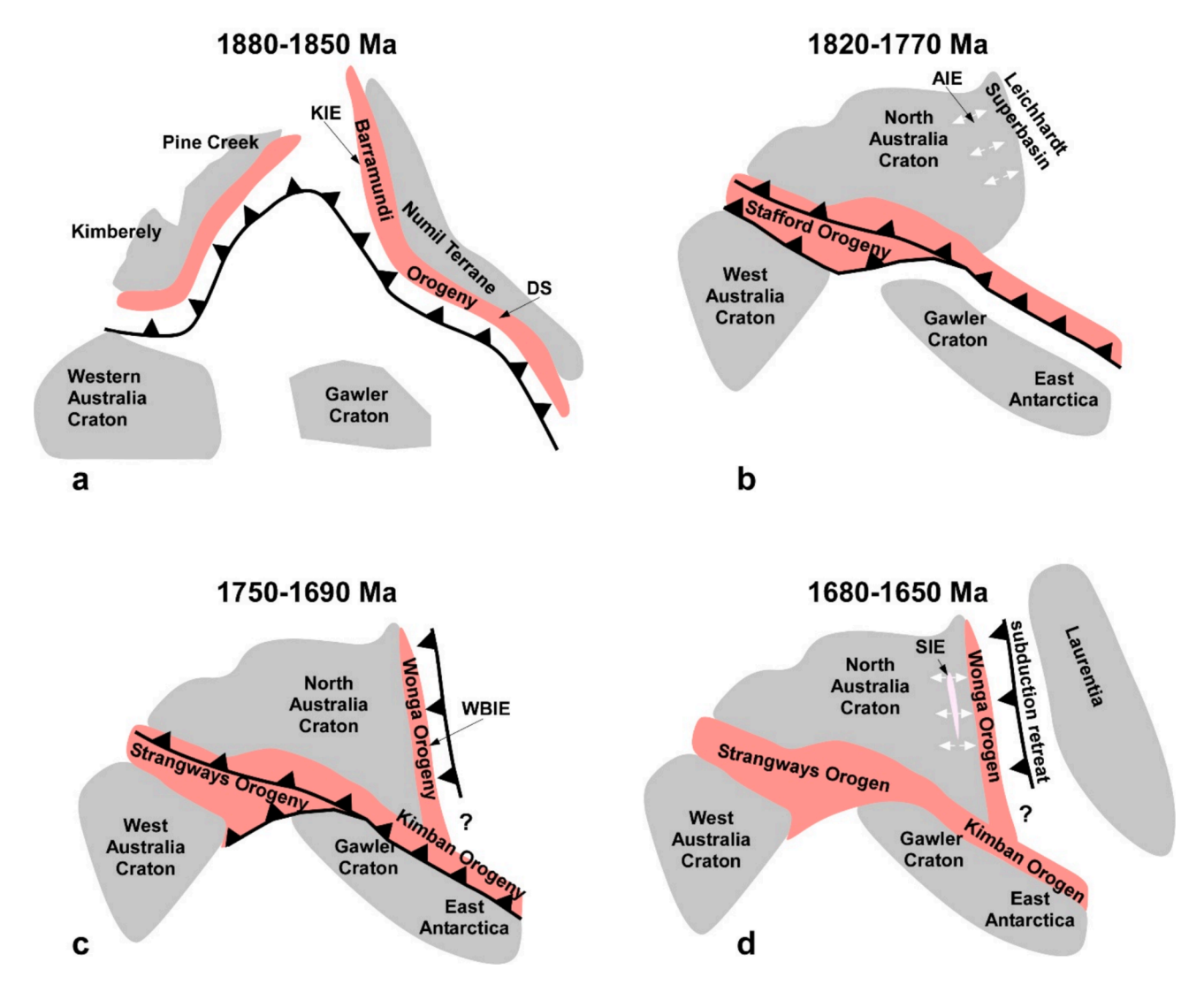


Fig. 11. Reconstruction models (modified from Betts & Giles, 2006; Gibson et al., 2025) to put in context the magmatic activity in Mount Isa Inlier for the period 1880 Ma to 1650 Ma and to illustrate some possible tectonic relationships with other Australian Proterozoic terranes during the final assembly of the Nuna Supercontinent. a) The Kalkadoon Igneous Event is in general interpret to occur along a continental margin during the Barramundi Orogeny and form a continuous belt with the Donington Suite in the SAC. b) In general, tectonic models indicate intracontinental extensional tectonics in Mount Isa Inlier during the period 1820 Ma to 1770 Ma in response to a far field subduction system along the southern margin of the NAC. However, as discussed in the text, new evidence suggests that at least some of this interpretation may require updating. c) The Wonga Orogeny and the Wonga-Burstall Igneous Event can be correlated to similar orogenic events in the SAC and along the southern margin of the NAC. It is possible that the Wonga-Burstall Igneous Event occurred in response to a west dipping subduction zone located east of the Mount Isa Inlier. d) The emplacement of the Sybella Igneous Event plutons is in synchronous with the opening of the Calvert Superbasin and is probably related to slab retreat and back-arc extension prior to the final collision with Laurentia at ca. 1600 Ma. KIE = Kalkadoon Igneous Event. AIE = Argylla Igneous Event. WBIE = Wonga-Burstall Igneous Event. SIE = Sybella Igneous Event.

region, the Camel Creek Granite intruded between ca. 1800 and 1784 Ma in the complexly deformed Bottletree formation whereas the Garden Creek Porphyry intruded at ca. 1783 Ma the deformed Mount Guide Quartzite (Fig. 3b). Further work is needed to confirm whether they intruded during deformation, or the deformation recorded in the Bottletree Formation, and the Mount Guide Quartzite predates the intrusion of these granites.

5.3.3. The 1750–1690 Ma Wonga-Burstall Igneous Event and the Wonga Orogeny

A series of intrusive rocks in the Dajarra region including the Steeles Granite, Copper Valley Granite and unnamed granites have emplacement ages between ca. 1710 and 1690 Ma (Table 1; Figs. 3c and e) which are slightly younger than the ca. 1750–1710 Ma Wonga orogeny as defined by Spence et al. (2022). Together with similar aged granites further north (i.e. Weberra Granite), the ca. 1710–1690 Ma granites

from Dajarra region define a north south trending belt sub-parallel to the intrusive belts emplaced during the Wonga orogeny in the eastern succession between ca. 1750–1710 Ma (Fig. 2). Spence et al. (2021, 2022) interpreted that the principal strain during the Wonga Orogeny occurred in the Eastern Succession with decreasing intensity of deformation in the western part of the inlier. We interpret that the younger, ca. 1710–1690 Ma granites, emplaced in the Western Succession represent the wanning stages of the Wonga Orogeny and may also indicate a western migration of the locus of tectonic activity in the Mount Isa Inlier (Fig. 11c). This westward migration of the locus of tectonic activity in the inlier is further supported by the emplacement of the voluminous Sybella batholith during the Sybella Igneous Event soon after the end of the Wonga Orogeny.

The Wonga Orogeny and the corresponding igneous activity can be correlated with the Strangways Orogeny and the Kimban Orogeny, recorded from the southern part of the NAC and along the eastern part of

the SAC, respectively. The Strangways Orogeny was documented between ca. 1740 and 1690 Ma (Claoué-Long et al., 2008; Collins & Shaw, 1995; Scrimgeour, 2013; Zhao & Bennett, 1995) and interpreted to have formed in response to a north dipping subduction zone located in the southern part of the NAC (Giles et al., 2002; Zhao et al., 2004; Zhao & McCulloch, 1995) whereas the Kimban Orogeny occurred between ca. 1730 and 1690 Ma (Dutch et al., 2008; Dutch et al., 2010; Hand et al., 2007; Payne et al., 2008; Reid & Hand, 2012; Reid et al., 2008b) in response to a northeast dipping subduction zone representing a continuation of the subduction system responsible for the Strangways Orogeny. One possible interpretation is that the magmatic and tectonic activity in Mount Isa Inlier are related to the subduction systems responsible for the Strangways and the Kimban Orogenies and represents a far field intraplate environment rather than a plate margin (e.g. Betts & Giles, 2006). An alternative interpretation suggests that a west dipping subduction system developed east of Mount Isa Inlier, represented by the Gidea Suture (Korsch et al., 2012), and was responsible for the tectonic and magmatic activity during the Wonga Orogeny (Spence et al., 2021). Based on similar orientation of tectonic fabrics, magmatic A-type affinity and zircon isotopic record, Olierook et al. (2022) proposed that during the Wonga and Kimban orogenies there was a continuum of the NAC and SAC during the amalgamation of Nuna. If that is the case, it is possible that the NAC and SAC shared a common driver for the tectonic activity along its eastern margin at least since the Wonga and Kimban Orogenies.

5.3.4. The 1680-1650 Ma Sybella Igneous Event

The Sybella Igneous Event occurs almost exclusively in the Western Succession and forms a north–south trending belt of granitoids (Fig. 2a). Our study has shown that most intrusions attributed to this event in the Dajarra region are actually older and the distribution of rocks of the Sybella Igneous Event are closely related to the vicinity of the Rufus-Mt Isa fault system. Actually, with the exception of one pluton from the southwestern part of the Dajarra region that appears to be located east of the Rufus-Mt Isa Fault System and all the igneous rocks belonging to this event are located west of this fault system (Fig. 3e). Since the exact geometry of the Rufus Fault in this part of the inlier is not clearly defined it is likely that this intrusion is also located west of the fault. If that is the case, the strong control of the Rufus-Mt Isa fault system on the locus of magmatic activity during the Sybella Igneous Event suggests that this fault system may represent a major crustal boundary.

The Sybella Igneous Event starts ~ 10 my after the Wonga-Burstall Igneous Event and the end of the Wonga Orogeny further confirming a westward shift of the igneous activity. In general, the emplacement of the granitoids related to the Sybella Igneous Event is interpreted to have occurred during crustal extension and opening of the Calvert Superbasin (Gibson et al., 2008, 2016). It could be related to slab retreat and back arc extension of the subduction system responsible for the Wonga Orogeny and the corresponding Wonga-Burstall Igneous Event as proposed by Spence et al. (2021) before the final closure of an eastward facing ocean and collision with Laurentia at ca. 1600 Ma (Pourteau et al., 2018) (Fig. 11d).

5.4. An active continental margin during Nuna assembly

The position of the NAC on various tectonic reconstruction models varies widely during the Paleoproterozoic (Elming et al., 2021 and reference therein) but most models indicate that its eastern margin was facing an ocean at least until ca. 1600 Ma when a collision with Laurentia is envisaged by some authors (Nordsvan et al., 2018). The Mount Isa Inlier forms a linear belt that is at least 700 Kms long in its present configuration. The Kalkadoon-Leichardt Belt is the oldest tectonic element and its continuity along the entire length of the inlier indicates that the current geometry of the inlier was already in place during the Kalkadoon Igneous Event and controlled the subsequent tectonic and magmatic activity. The granites and granodiorites emplaced during the

Kalkadoon Igneous Event have an I-type character and their geochemical signature is similar to modern continental arc magmas (Bierlein et al., 2011; Wyborn et al., 1992) indicating an active continental margin from the onset of tectonic activity. The subsequent Argylla, Burstall-Wonga, Sybella and Williams igneous events produced plutons distributed in sub-parallel magmatic belts following the earlier established geometry in a similar way to modern day active continental margins. However, following the Kalkadoon Igneous Event all the subsequent magmatic events are dominated by A-type magmatism (Wyborn, 1988; Wyborn et al., 1992) which is different from the typical calc-alkaline magmatism occurring along modern active continental margins. This can be attributed to hotter Proterozoic orogens which favoured the generation of voluminous A-type magmatism globally during the Proterozoic (Spencer et al., 2021). Nordsvan et al. (2022) proposed that the Mount Isa Inlier is similar to retreating orogens such as the Paleozoic Lachlan Orogenic Belt along the eastern coast of Australia where magmatism was active over a protracted period. The isotopic data from the Lachlan Orogenic Belt indicates that periods of crustal reworking alternated with periods of juvenile crust input corresponding to back arc closure and opening events in response to complex subduction dynamics involving alternating periods of slab retreat and advance (Kemp et al., 2009b). In contrast, Hf isotope data (Fig. 9 and Fig. 10) from Mount Isa indicates that crustal reworking was the dominant mechanism of crustal growth through most of its almost 400 Myr of magmatic history. This could indicate a thicker crust, a possible Archean-Paleoproterozoic core (Kerr et al., 2024), and/or a more limited back-arc extension which favoured heating of the crust to produce A-type magmatism but inhibited the ascend of mantle derived magmas which most likely pondered in the lower crust. In general Mount Isa Inlier shows many similar characteristics to modern, active continental margins but with typical Proterozoic affinities such as voluminous A-type magmatism and higher thermal gradients.

6. Conclusion

New U-Pb zircon geochronological data from granitic intrusions in the Dajarra region reveal the presence of four distinct magmatic events in the southern part of the Western Fold Belt, Mount Isa Inlier: the Kalkadoon Igneous Event (ca. 1880-1850 Ma), the Argylla Igneous Event (ca. 1820-1770 Ma), the Wonga-Burstall Igneous Event (ca. 1750-1690 Ma), and the Sybella Igneous Event (ca. 1680-1650 Ma). These events occur as a series of sub-parallel, north-south trending magmatic belts that extend across almost the entire length of the inlier. The Hf isotopic data show that most of these granites were formed by crustal reworking and there is limited evidence of juvenile crustal input. The new ages and the Hf isotope data are consistent with the igneous evolution recorded across the inlier and points to a tectonic and magmatic evolution dominated by episodic reworking of an active continental margin. The new ages, particularly the age of the Garden Creek Porphyry and the Camel Creek Granite have significant implications for the stratigraphy of the Western Succession and suggests that the stratigraphic framework needs refining. Notably, our results emphasize that the Argylla Igneous Event (ca. 1820 to 1770 Ma) can now be considered an inlier wide intrusive event forming a series of two subparallel magmatic belts that can be correlated with similar magmatic activity in other parts of the NAC. We consider that the ca. 1710-1690 Ma intrusive from the WFB are part of the Wonga-Burstall Igneous Event and represent a westward shift in magmatic activity during the waning stages of the Wonga Orogeny. Overall, the new data provides improved spatial and temporal correlations of magmatic belts spanning between ca. 1880 and 1650 Ma across both the North Australian Craton (NAC) and the South Australian Craton (SAC) and will help better understand models leading to paleogeographic reconstruction and supercontinent assembly processes.

CRediT authorship contribution statement

Sutthida Noptalung: Writing – original draft, Visualization, Methodology, Investigation, Formal analysis, Data curation, Conceptualization. **Ioan V. Sanislav:** Writing – review & editing, Validation, Supervision, Investigation, Funding acquisition, Conceptualization. **Helen A. Cocker:** Writing – review & editing. **Avish Kumar:** Writing – review & editing.

Declaration of competing interest

The authors declare that they have no known competing financial interests or personal relationships that could have appeared to influence the work reported in this paper.

Acknowledgements

This study is part of a PhD project conducted by the first author, Sutthida Noptalung, at James Cook University. The first author would like to acknowledge funding from the Institute for the Promotion of Teaching Science and Technology (Thailand) and the Economic Geology Research Centre (EGRU) at James Cook University (Townsville, Australia). Alanis Olesch-Byrne is thanked for helping with fieldwork, sample collection and for being a great colleague.

Appendix A. Supplementary data

Supplementary data to this article can be found online at https://doi.org/10.1016/j.precamres.2025.107965.

Data availability

Data will be made available on request.

References

- Abu Sharib, A.S.A.A., Sanislav, I.V., 2013. Polymetamorphism accompanied switching in horizontal shortening during Isan Orogeny: example from the Eastern Fold Belt, Mount Isa Inlier, Australia. Tectonophysics 587, 146–167. https://doi.org/10.1016/i.tecto.2012.06.051.
- Bagas, L., Bierlein, F.P., Anderson, J.A.C., Maas, R., 2010. Collision-related granitic magmatism in the Granites-Tanami Orogen. Western Australia. Precambrian Research 177 (1), 212–226. https://doi.org/10.1016/j.precamres.2009.12.002.
- Betts, P.G., 1999. Palaeoproterozoic mid-basin inversion in the northern Mt Isa terrane. Queensland. Australian Journal of Earth Sciences 46 (5), 735–748. https://doi.org/ 10.1046/j.1440-0952.1999.00741.x.
- Betts, P.G., Giles, D., 2006. The 1800–1100 Ma tectonic evolution of Australia. Precambr. Res. 144 (1), 92–125. https://doi.org/10.1016/j.precamres.2005.11.006.
- Betts, P.G., Giles, D., Mark, G., Lister, G.S., Goleby, B.R., Aillères, L., 2006. Synthesis of the proterozoic evolution of the Mt Isa Inlier. Aust. J. Earth Sci. 53 (1), 187–211. https://doi.org/10.1080/08120090500434625.
- Betts, P.G., Giles, D., Foden, J., Schaefer, B.F., Mark, G., Pankhurst, M.J., Forbes, C.J., Williams, H.A., Chalmers, N.C., Hills, Q., 2009. Mesoproterozoic plume-modified orogenesis in eastern Precambrian Australia. Tectonics 28 (3). https://doi.org/ 10.1029/2008TC002325.
- Betts, P.G., Armit, R.J., Stewart, J., Aitken, A.R.A., Ailleres, L., Donchak, P., Hutton, L., Withnall, I., Giles, D., 2016. Australia and Nuna. Geol. Soc. Lond. Spec. Publ. 424 (1), 47–81. https://doi.org/10.1144/SP424.2.
- Bierlein, F.P., Black, L.P., Hergt;, J., Mark, G., 2008. Evolution of Pre-1.8 Ga basement rocks in the western Mt Isa Inlier, northeastern Australia—Insights from SHRIMP U-Pb dating and in-situ Lu-Hf analysis of zircons. Precambr. Res. 163 (1), 159–173. https://doi.org/10.1016/j.precamres.2007.08.017.
- Bierlein, F.P., Maas, R., Woodhead, J., 2011. Pre-1.8 Ga tectono-magmatic evolution of the Kalkadoon–Leichhardt Belt: Implications for the crustal architecture and metallogeny of the Mount Isa Inlier, northwest Queensland, Australia. Aust. J. Earth Sci. 58 (8), 887–915. https://doi.org/10.1080/08120099.2011.571286.
- Black, L.P., Kamo, S.L., Allen, C.M., Aleinikoff, J.N., Davis, D.W., Korsch, R.J., Foudoulis, C., 2003. TEMORA 1: a new zircon standard for Phanerozoic U-Pb geochronology. Chem. Geol. 200 (1), 155–170. https://doi.org/10.1016/S0009-2541(03)00165-7
- Blaikie, T.N., Betts, P.G., Armit, R.J., Ailleres, L., 2017. The ca. 1740–1710 Ma Leichhardt Event: Inversion of a continental rift and revision of the tectonic evolution of the North Australian Craton. Precambr. Res. 292, 75–92. https://doi. org/10.1016/j.precamres.2017.02.003.

- Blake, D.H., 1980. The early geological history of the Proterozoic Mount Isa Inlier, northwestern Queensland: an alternative interpretation. BMR J. Aust. Geol. Geophys. 5 (4), 243–256.
- Blake, D.H., 1987. Geology of the Mount Isa Inlier and environs, Queensland and Northern Territory. Bureau of Mineral Resources, Geology and Geophysics, Australia, Bulletin 225, 1–83.
- Blake, D. H., & Stewart, A. J. (1992). Stratigraphic and tectonic framework, Mount Isa Inlier. In Stewart A. J. & D. H. Blake (Eds.), *Detailed studies of the Mount Isa Inlier* (pp. 1–11). Australian Geological Survey Organisation Bulletin 243.
- Blake, D.H., Bultitude, R.J., Donchak, P.J.T., 1982. Dajarra 1:100000 Geological Map Commentary. Bureau of Mineral Resources, Geology, Geophysics.
- Blake, D.H., Bultitude, R.J., Donchak, P.J.T., Wyborn, L.A.I., Hone, I.G., 1984. Geology of the Duchess-Urandangi region, Mount Isa Inlier, Queensland. Bureau of Mineral Resources, Geology and Geophysics, Australia, Bulletin 219, 1–91.
- Bonin, B., 1990. From orogenic to anorogenic settings: Evolution of granitoid suites after a major orogenesis. Geol. J. 25 (3–4), 261–270. https://doi.org/10.1002/ gi.3350250309.
- Bouvier, A., Vervoort, J.D., Patchett, P.J., 2008. The Lu–Hf and Sm–Nd isotopic composition of CHUR: Constraints from unequilibrated chondrites and implications for the bulk composition of terrestrial planets. Earth Planet. Sci. Lett. 273 (1), 48–57. https://doi.org/10.1016/j.epsl.2008.06.010.
- Brown, A., Spandler, C., Blenkinsop, T.G., 2023. New age constraints for the Tommy Creek Domain of the Mount Isa Inlier. Australia. Australian Journal of Earth Sciences 70 (3), 358–374. https://doi.org/10.1080/08120099.2023.2171124.
- Bultitude, R.J., 1982. Ardmore 1:100000 Geological Map Commentary. Bureau of Mineral Resources, Geology, Geophysics.
- Bultitude, R.J., Purdy, D.J., Brown, D.D., Hoy, D., 2021. Igneous Geology of the Mary Kathleen Domain (MKD). Queensland Geological Record 2021 (02).
- Carson, C.J., Hutton, L.J., Withnall, I.W., Perkins, W.G., 2009. Joint GSQ-GA NGA geochronology project, Mount Isa region, 2007–2008. Queensland Geological Record 2008 (05).
- Carson, C.J., Hutton, L.J., Withnall, I.W., Perkins, W.J., Donchak, P.J.T., Parsons, A., Blake, P.R., Sweet, I.P., Neumann, N.L., Lambeck, A., 2011. Joint GSQ-GA NGA geochronology project, Mount Isa region, 2009–2010. Queensland Geological Record 2011 (03).
- Cawood, P.A., Korsch, R.J., 2008. Assembling Australia: Proterozoic building of a continent. Precambr. Res. 166 (1), 1–35. https://doi.org/10.1016/j. precampres.2008.08.006.
- Claoué-Long, J., Edgoose, C., 2008. The age and significance of the Ngadarunga Granite in Proterozoic central Australia. Precambr. Res. 166 (1), 219–229. https://doi.org/ 10.1016/j.precamres.2007.06.026.
- Claoué-Long, J., Maidment, D., Hussey, K., Huston, D., 2008. The duration of the Strangways Event in central Australia: evidence for prolonged deep crust processes. Precambr. Res. 166 (1), 246–262. https://doi.org/10.1016/j. precamres.2007.06.023.
- Cocker, H.A., Sanislav, I., Dirks, P., McCoy-West, A., 2025. Zircon U–Pb emplacement ages of intrusions in the Mary Kathleen Domain, Mount Isa Inlier. Australia. Australian Journal of Earth Sciences 1–25. https://doi.org/10.1080/ 08120099.2025.2527816.
- Collins, W.J., Shaw, R.D., 1995. Geochronological constraints on orogenic events in the Arunta Inlier: a review. Precambr. Res. 71 (1), 315–346. https://doi.org/10.1016/ 0301-9268(94)00067-2.
- Connors, K.A., Page, R.W., 1995. Relationships between magmatism, metamorphism and deformation in the western Mount Isa Inlier. Australia. Precambrian Research 71 (1), 131–153. https://doi.org/10.1016/0301-9268(94)00059-Z.
- Crispe, A.J., Vandenberg, L.C., Scrimgeour, I.R., 2007. Geological framework of the Archean and Paleoproterozoic Tanami Region. Northern Territory. Mineralium Deposita 42 (1), 3–26. https://doi.org/10.1007/s00126-006-0107-1.
- Derrick, G.M., 1982. A Proterozoic rift zone at Mount Isa, Queensland, and implications for mineralisation. BMR J. Aust. Geol. Geophys. 7 (2), 81–92.
- Derrick, G.M., Wilson, I.H., Hill, R.M., Glikson, A.Y., Mitchell, J.E., 1977. Geology of the Mary Kathleen 1:100 000 Sheet area, northwest Queensland. Bureau of Mineral Resources, Geology, Geophysics
- Dutch, R., Hand, M., Kinny, P.D., 2008. High-grade Paleoproterozoic reworking in the southeastern Gawler Craton, South Australia *. Aust. J. Earth Sci. 55 (8), 1063–1081. https://doi.org/10.1080/08120090802266550.
- Dutch, R.A., Hand, M., Kelsey, D.E., 2010. Unravelling the tectonothermal evolution of reworked Archean granulite facies metapelites using in situ geochronology: an example from the Gawler Craton. Australia. Journal of Metamorphic Geology 28 (3), 293–316. https://doi.org/10.1111/j.1525-1314.2010.00867.x.
- Elming, S.-Å., Salminen, J., & Pesonen, L. J. (2021). Chapter 16—Paleo-Mesoproterozoic Nuna supercycle. In L. J. Pesonen, J. Salminen, S.-Å. Elming, D. A. D. Evans, & T. Veikkolainen (Eds.), Ancient Supercontinents and the Paleogeography of Earth (pp. 499–548). Elsevier. Doi: 10.1016/B978-0-12-818533-9.00001-1.
- Eriksson, K.A., Simpson, E.L., 1993. Siliciclastic Braided-Alluvial Sediments Intercalated within Continental Flood Basalts in the Early to Middle Proterozoic Mount Isa Inlier, Australia. In: Marzo, M., Puigdefábregas, C. (Eds.), *Alluvial Sedimentation*. John Wiley & Sons, Ltd, pp. 473–488. https://doi.org/10.1002/9781444303995.ch30.
- Etheridge, M.A., Rutland, R.W.R., Wyborn, L.A., 1987. Orogenesis and tectonic process in the Early to Middle Proterozoic of northern Australia. In: Kröner, A. (Ed.), Proterozic Lithospheric Evolution. American Geophysical Union Geodynamics Series 17, pp. 131–147.
- Foster, D.R.W., Austin, J.R., 2008. The 1800–1610 Ma stratigraphic and magmatic history of the Eastern Succession, Mount Isa Inlier, and correlations with adjacent Paleoproterozoic terranes. Precambr. Res. 163 (1), 7–30. https://doi.org/10.1016/j. precamres.2007.08.010.

- Foster, D.R.W., Rubenach, M.J., 2006. Isograd pattern and regional low-pressure, high-temperature metamorphism of pelitic, mafic and calc-silicate rocks along an east west section through the Mt Isa Inlier. Aust. J. Earth Sci. 53 (1), 167–186. https://doi.org/10.1080/08120090500434617.
- Geological Survey of Queensland. (2011). Proterozoic Geological Domains. In *North-West Queensland Mineral and Energy Province Report* (pp. 6–22). Queensland Department of Employment, Economic Development and Innovation.
- Gibson, G.M., Rubenach, M.J., Neumann, N.L., Southgate, P.N., Hutton, L.J., 2008. Synand post-extensional tectonic activity in the Palaeoproterozoic sequences of Broken Hill and Mount Isa and its bearing on reconstructions of Rodinia. Precambr. Res. 166 (1), 350–369. https://doi.org/10.1016/j.precamres.2007.05.005.
- Gibson, G.M., Meixner, A.J., Withnall, I.W., Korsch, R.J., Hutton, L.J., Jones, L.E.A., Holzschuh, J., Costelloe, R.D., Henson, P.A., Saygin, E., 2016. Basin architecture and evolution in the Mount Isa mineral province, northern Australia: Constraints from deep seismic reflection profiling and implications for ore genesis. Ore Geol. Rev. 76, 414-441. https://doi.org/10.1016/j.oregeorev.2015.07.013.
- Gibson, G.M., Champion, D.C., Doublier, M.P., 2025. The Paleoproterozoic Trans-Australian Orogen: its magmatic and tectonothermal record, links to northern Laurentia, and implications for supercontinent assembly. GSA Bull. 137 (1–2), 495–521. https://doi.org/10.1130/B36255.1.
- Giles, D., Betts, P., & Lister, G. (2002). Far-field continental backarc setting for the 1.80–1.67 Ga basins of northeastern Australia. *Geology*, 30(9), 823–826. Doi: 10.1130/0091-7613(2002)030<0823:FFCBSF>2.0.CO;2.
- Hand, M., & Buick, I. S. (2001). Tectonic evolution of the Reynolds–Anmatjira Ranges: A case study in terrain reworking from the Arunta Inlier, central Australia. In J. A. Miller, R. E. Holdsworth, I. S. Buick, & M. Hand (Eds.), Continental Reactivation and Reworking (Vol. 184, p. 0). Geological Society of London. Doi: 10.1144/GSL. SP.2001.184.01.12.
- Hand, M., Reid, A., Jagodzinski, L., 2007. Tectonic Framework and Evolution of the Gawler Craton. Southern Australia. Economic Geology 102 (8), 1377–1395. https:// doi.org/10.2113/gsecongeo.102.8.1377.
- Horstwood, M.S.A., Košler, J., Gehrels, G., Jackson, S.E., McLean, N.M., Paton, C., Pearson, N.J., Sircombe, K., Sylvester, P., Vermeesch, P., Bowring, J.F., Condon, D.J., Schoene, B., 2016. Community-Derived Standards for LA-ICP-MS U-(Th-)Pb Geochronology – uncertainty Propagation, Age Interpretation and Data Reporting. Geostand. Geoanal. Res. 40 (3), 311–332. https://doi.org/10.1111/j.1751-908X.2016.00379.x.
- Howlett, D., Raimondo, T., Hand, M., 2015. Evidence for 1808–1770 Ma bimodal magmatism, sedimentation, high-temperature deformation and metamorphism in the Aileron Province, central Australia. Aust. J. Earth Sci. 62 (7), 831–852. https:// doi.org/10.1080/08120099.2015.1108364.
- Iaccheri, L.M., 2019. Composite basement along the southern margin of the North Australian Craton: evidence from in-situ zircon U-Pb-O-Hf and whole-rock Nd isotopic compositions. Lithos 324–325, 733–746. https://doi.org/10.1016/j. lithos.2018.11.006.
- Jackson, M.J., Scott, D.L., Rawlings, D.J., 2000. Stratigraphic framework for the Leichhardt and Calvert Superbasins: Review and correlations of the pre-1700 Ma successions between Mt Isa and McArthur River. Aust. J. Earth Sci. 47 (3), 381–403. https://doi.org/10.1046/j.1440-0952.2000.00789.x.
- Jackson, S.E., Pearson, N.J., Griffin, W.L., Belousova, E.A., 2004. The application of laser ablation-inductively coupled plasma-mass spectrometry to in situ U–Pb zircon geochronology. Chem. Geol. 211 (1), 47–69. https://doi.org/10.1016/j. chem.ep. 2004.06.017
- Kemp, A.I.S., Foster, G.L., Scherstén, A., Whitehouse, M.J., Darling, J., Storey, C., 2009a. Concurrent Pb-Hf isotope analysis of zircon by laser ablation multi-collector ICP-MS, with implications for the crustal evolution of Greenland and the Himalayas. Chem. Cod. 251 (2), 244, 260. https://doi.org/10.1016/j.chempeg.2008.06.018
- Geol. 261 (3), 244–260. https://doi.org/10.1016/j.chemgeo.2008.06.019.
 Kemp, A.I.S., Hawkesworth, C.J., Collins, W.J., Gray, C.M., Blevin, P.L., 2009b. Isotopic evidence for rapid continental growth in an extensional accretionary orogen: the Tasmanides, eastern Australia. Earth Planet. Sci. Lett. 284 (3), 455–466. https://doi.org/10.1016/j.epsl.2009.05.011.
- Kerr, J.M., Brown, D.D., Connors, K.A., Heinson, G., 2024. Electrical structure and crustal architecture of the southern Mount Isa Province. Explor. Geophys. 55 (5), 530–544. https://doi.org/10.1080/08123985.2023.2291482.
- Korsch, R.J., Huston, D.L., Henderson, R.A., Blewett, R.S., Withnall, I.W., Fergusson, C. L., Collins, W.J., Saygin, E., Kositcin, N., Meixner, A.J., Chopping, R., Henson, P.A., Champion, D.C., Hutton, L.J., Wormald, R., Holzschuh, J., Costelloe, R.D., 2012. Crustal architecture and geodynamics of North Queensland, Australia: Insights from deep seismic reflection profiling. Tectonophysics 572–573, 76–99. https://doi.org/10.1016/j.tecto.2012.02.022.
- Le, T.X., Dirks, P.H.G.M., Sanislav, I.V., Huizenga, J.M., Cocker, H.A., Manestar, G.N., 2021a. Geochronological constraints on the geological history and gold mineralization in the Tick Hill region. Mt Isa Inlier. Precambrian Research 366, 106422. https://doi.org/10.1016/j.precamres.2021.106422.
- Le, T.X., Dirks, P.H.G.M., Sanislav, I.V., Huizenga, J.M., Cocker, H.A., Manestar, G.N., 2021b. Geological setting and mineralization characteristics of the Tick Hill Gold Deposit, Mount Isa Inlier, Queensland, Australia. Ore Geology Reviews 137, 104288. https://doi.org/10.1016/j.oregeorev.2021.104288.
- Le, T.X., Dirks, P.H.G.M., Sanislav, I.V., Huizenga, J.M., Cocker, H.A., Nguyen, G.T.T., 2024. P-T conditions of metamorphic and hydrothermal events at Tick Hill Gold Deposit, Mount Isa, Queensland, Australia. Australian Journal of Earth Sciences 71 (4), 538-552. https://doi.org/10.1080/08120099.2024.2320195.
- Lewis, C.J., Bultitude, R.J., Hutton, L.J., Waltenberg, K., Armstrong, R.A., Evans, N.J., 2022. Unravelling the pre-1860–1850 Ma 'basement' history of the Mount Isa Inlier. Geoscience Australia. https://doi.org/10.26186/120990.

- Li, S., Chung, S.-L., Wilde, S.A., Wang, T., Xiao, W.-J., Guo, Q.-Q., 2016. Linking magmatism with collision in an accretionary orogen. Sci. Rep. 6 (1), 25751. https:// doi.org/10.1038/srep.25751
- MacCready, T., Goleby, B.R., Goncharov, A., Drummond, B.J., Lister, G.S., 1998.
 A framework of overprinting orogens based on interpretation of the Mount Isa deep seismic transect. Econ. Geol. 93 (8), 1422–1434. https://doi.org/10.2113/gsecongeo.93.8.1422.
- Magee, C.W., Withnall, I.W., Hutton, L.J., Perkins, W.J., Donchak, P.J.T., Parson, A., Blake, P.R., Sweet, I.P., Carson, C.J., 2012. Joint GSQ–GA geochronology project, Mount Isa Region, 2008–2009. Queensland Geological Record 2012 (07).
- McDonald, G. D., Collerson, K. D., & Kinny, P. D. (1997). Late Archean and Early Proterozoic crustal evolution of the Mount Isa block, northwest Queensland, Australia. *Geology*, 25(12), 1095–1098. Doi: 10.1130/0091-7613(1997)025<1095: LAAEPC>2.3.CO:2.
- Neumann, N.L., Southgate, P.N., Gibson, G.M., MCintyre, A., 2006. New SHRIMP geochronology for the Western Fold Belt of the Mt Isa Inlier: developing a 1800–1650 Ma event framework. Aust. J. Earth Sci. 53 (6), 1023–1039. https://doi.org/10.1080/08120090600923287.
- Neumann, N.L., Gibson, G.M., Southgate, P.N., 2009. New SHRIMP age constraints on the timing and duration of magmatism and sedimentation in the Mary Kathleen Fold Belt, Mt Isa Inlier. Australia. Australian Journal of Earth Sciences 56 (7), 965–983. https://doi.org/10.1080/08120090903005410.
- Nordsvan, A.R., Collins, W.J., Li, Z.-X., Spencer, C.J., Pourteau, A., Withnall, I.W., Betts, P.G., Volante, S., 2018. Laurentian crust in northeast Australia: Implications for the assembly of the supercontinent Nuna. Geology 46 (3), 251–254. https://doi. org/10.1130/G39980.1.
- Nordsvan, A.R., Volante, S., Collins, W.J., Pourteau, A., Li, J., Withnall, I.W., Beams, S., Li, Z.-X., 2022. Post-collisional magmatism in NE Australia during Mesoproterozoic supercontinent Nuna: Insights from new zircon UPb and LuHf data. Lithos 428–429, 106827. https://doi.org/10.1016/j.lithos.2022.106827.
- Olierook, H.K.H., Mervine, E.M., Armstrong, R., Duckworth, R., Evans, N.J., McDonald, B., Kirkland, C.L., Shantha Kumara, A., Wood, D.G., Cristall, J., Jhala, K., Stirling, D.A., Friedman, I., McInnes, B.I.A., 2022. Uncovering the Leichhardt Superbasin and Kalkadoon-Leichhardt complex in the southern Mount Isa Terrane. Australia. Precambrian Research 375, 106680. https://doi.org/10.1016/j.precamres.2022.106680.
- Oliver, N.H.S., Holcombe, R.J., Hill, E.J., Pearson, P.J., 1991. Tectono-metamorphic evolution of the Mary Kathleen fold belt, northwest Queensland: a reflection of mantle plume processes? Aust. J. Earth Sci. 38 (4), 425–455. https://doi.org/10.1080/08120099108727982.
- O'Dea, M.G., Lister, G.S., Betts, P.G., Pound, K.S., 1997a. A shortened intraplate rift system in the Proterozoic Mount Isa terrane, NW Queensland. Australia. Tectonics 16 (3), 425–441. https://doi.org/10.1029/96TC03276.
- O'Dea, M.G., Lister, G.S., Maccready, T., Betts, P.G., Oliver, N.H.S., Pound, K.S., Huang, W., Valenta, R.K., Oliver, N.H.S., Valenta, R.K., 1997b. Geodynamic evolution of the Proterozoic Mount Isa terrain. Geol. Soc. Lond. Spec. Publ. 121 (1), 99–122. https://doi.org/10.1144/GSL.SP.1997.121.01.05.
- Paces, J.B., Miller Jr., J.D., 1993. Precise U-Pb ages of Duluth complex and related maficintrusions, northeastern Minnesota: Geochronological insights to physical, petrogenetic, paleomagnetic, and tectonomagnatic processes associated with the 1.1 Ga Midcontinent Rift System. J. Geophys. Res. Solid Earth 98 (B8), 13997–14013. https://doi.org/10.1029/93JB01159.
- Page, R.W., 1978. Response of U-Pb Zircon and Rb-Sr total-rock and mineral systems to low-grade regional metamorphism in proterozoic igneous rocks, mount Isa, Australia. J. Geol. Soc. Aust. 25 (3–4), 141–164. https://doi.org/10.1080/ 00167617808729025.
- Page, R.W., 1983. Timing of superposed volcanism in the Proterozoic Mount Isa Inlier. Australia. Precambrian Research 21 (3), 223–245. https://doi.org/10.1016/0301-9268(83)90042-6.
- Page, R.W., Sun, S., 1998. Aspects of geochronology and crustal evolution in the Eastern Fold Belt, Mt Isa Inlier. Aust. J. Earth Sci. 45 (3), 343–361. https://doi.org/10.1080/ 08120099808728396.
- Page, R.W., Williams, I.S., 1988. Age of the barramundi orogeny in northern Australia by means of ion microprobe and conventional U-Pb zircon studies. Precambr. Res. 40–41, 21–36. https://doi.org/10.1016/0301-9268(88)90059-9.
- Page, R.W., Griffin, T.J., Tyler, I.M., Sheppard, S., 2001. Geochronological constraints on tectonic models for Australian Palaeoproterozoic high-K granites. J. Geol. Soc. London 158 (3), 535–545. https://doi.org/10.1144/jgs.158.3.535.
- Passchier, C.W., Williams, P.R., 1989. Proterozoic extensional deformation in the Mount Isa inlier, Queensland. Australia. Geological Magazine 126 (1), 43–53. https://doi. org/10.1017/S0016756800006130.
- Paton, C., Hellstrom, J., Paul, B., Woodhead, J., Hergt;, J., 2011. Iolite: Freeware for the visualisation and processing of mass spectrometric data. J. Anal. At. Spectrom 26 (12), 2508. https://doi.org/10.1039/c1ja10172b.
- Payne, J.L., Hand, M., Barovich, K.M., Wade, B.P., 2008. Temporal constraints on the timing of high-grade metamorphism in the northern Gawler Craton: Implications for assembly of the Australian Proterozoic. Aust. J. Earth Sci. 55 (5), 623–640. https:// doi.org/10.1080/08120090801982595.
- Pourteau, A., Smit, M.A., Li, Z.-X., Collins, W.J., Nordsvan, A.R., Volante, S., Li, J., 2018. 1.6 Ga crustal thickening along the final Nuna suture. Geology 46 (11), 959–962. https://doi.org/10.1130/G45198.1.
- Reid, A.J., Hand, M., 2012. Mesoarchean to Mesoproterozoic evolution of the southern Gawler Craton. South Australia. Episodes 35 (1), 216–225. https://doi.org/ 10.18814/epiiugs/2012/v35i1/021.

- Reid, A., Hand, M., Jagodzinski, E., Kelsey, D., Pearson, N., 2008a. Paleoproterozoic orogenesis in the southeastern Gawler Craton, South Australia. Aust. J. Earth Sci. 55 (4), 449–471. https://doi.org/10.1080/08120090801888594.
- Reid, A.J., McAvaney, S.O., Fraser, G.L., 2008b. Nature of the Kimban Orogeny across northern Eyre Peninsula. MESA Journal 51, 25–34.
- Scott, D.L., Rawlings, D.J., Page, R.W., Tarlowski, C.Z., Idnurm, M., Jackson, M.J., Southgate, P.N., 2000. Basement framework and geodynamic evolution of the Palaeoproterozoic superbasins of north-central Australia: an integrated review of geochemical, geochronological and geophysical data. Aust. J. Earth Sci. 47 (3), 341–380. https://doi.org/10.1046/j.1440-0952.2000.00793.x.
- Scrimgeour, I. R. (2013). Chapter 12: Aileron Province. In M. Ahmad & T. J. Munson, Geology and mineral resources of the Northern Territory. Northern Territory Geological Survey, Special Publication 5.
- Sláma, J., Košler, J., Condon, D.J., Crowley, J.L., Gerdes, A., Hanchar, J.M., Horstwood, M.S.A., Morris, G.A., Nasdala, L., Norberg, N., Schaltegger, U., Schoene, B., Tubrett, M.N., Whitehouse, M.J., 2008. Plešovice zircon—A new natural reference material for U–Pb and Hf isotopic microanalysis. Chem. Geol. 249 (1), 1–35. https://doi.org/10.1016/j.chemgeo.2007.11.005.
- Söderlund, U., Patchett, P.J., Vervoort, J.D., Isachsen, C.E., 2004. The 176Lu decay constant determined by Lu–Hf and U–Pb isotope systematics of Precambrian mafic intrusions. Earth Planet. Sci. Lett. 219 (3), 311–324. https://doi.org/10.1016/S0012-821X(04)00012-3.
- Spampinato, G.P.T., Betts, P.G., Ailleres, L., Armit, R.J., 2015. Structural architecture of the southern Mount Isa terrane in Queensland inferred from magnetic and gravity data. Precambr. Res. 269, 261–280. https://doi.org/10.1016/j. precampre 2015.08.017
- Spence, J.S., Sanislav, I.V., Dirks, P.H.G.M., 2021. 1750–1710 Ma deformation along the eastern margin of the North Australia Craton. Precambr. Res. 353, 106019. https:// doi.org/10.1016/j.precamres.2020.106019.
- Spence, J.S., Sanislav, I.V., Dirks, P.H.G.M., 2022. Evidence for a 1750–1710 Ma orogenic event, the Wonga Orogeny, in the Mount Isa Inlier, Australia: Implications for the tectonic evolution of the North Australian Craton and Nuna Supercontinent. Precambr. Res. 369, 106510. https://doi.org/10.1016/j.precamres.2021.106510.
- Spencer, C.J., Kirkland, C.L., Roberts, N.M.W., Evans, N.J., Liebmann, J., 2020. Strategies towards robust interpretations of in situ zircon Lu-Hf isotope analyses. Geosci. Front. 11 (3), 843–853. https://doi.org/10.1016/j.gsf.2019.09.004.
- Spencer, C.J., Mitchell, R.N., Brown, M., 2021. Enigmatic Mid-Proterozoic Orogens: Hot, thin, and Low. Geophys. Res. Lett. 48 (16), e2021GL093312. https://doi.org/10.1029/2021GL093312.
- Tichomirowa, M., Käßner, A., Sperner, B., Lapp, M., Leonhardt, D., Linnemann, U., Münker, C., Ovtcharova, M., Pfänder, J.A., Schaltegger, U., Sergeev, S., von Quadt, A., Whitehouse, M., 2019. Dating multiply overprinted granites: the effect of protracted magmatism and fluid flow on dating systems (zircon U-Pb: SHRIMP/SIMS, LA-ICP-MS, CA-ID-TIMS; and Rb-Sr, Ar-Ar) Granites from the Western Erzgebirge (Bohemian Massif, Germany). Chem. Geol. 519, 11–38. https://doi.org/10.1016/j.chemgeo.2019.04.024.
- Vermeesch, P., 2018. IsoplotR: a free and open toolbox for geochronology. Geosci. Front. 9 (5), 1479–1493. https://doi.org/10.1016/j.gsf.2018.04.001.

- Vervoort, J.D., Blichert-Toft, J., 1999. Evolution of the depleted mantle: Hf isotope evidence from juvenile rocks through time. Geochim. Cosmochim. Acta 63 (3), 533–556. https://doi.org/10.1016/S0016-7037(98)00274-9.
- Wiedenbeck, M., Allé, P., Corfu, F., Griffin, W. I., Meier, M., Oberli, F., Quadt, A. V., Roddick, J. c., & Spiegel, W. (1995). Three Natural Zircon Standards for U-Th-Pb, Lu-Hf, Trace Element and Ree Analyses. *Geostandards Newsletter*, 19(1), 1–23. Doi: 10.1111/j.1751-908X.1995.tb00147.x.
- Wilson, C.J.L., 1975. Structural features west of Mount Isa. J. Geol. Soc. Aust. 22 (4), 457–476. https://doi.org/10.1080/00167617508728911.
- Withnall, I.W., 2019. Review of SHRIMP zircon ages for the Eastern Succession of the Mount Isa Province and magmatic events in its provenance. Department of Natural Resources, Mines and Energy, Queensland.
- Withnall, I.W., Hutton, L.J., 2013. North Australian Craton. In: Jell, P.A. (Ed.), *Geology of Queensland*. Geological Survey of Queensland, pp. 23–112.
- Woodhead, J.D., Hergt;, J.M., 2005. A Preliminary Appraisal of Seven Natural Zircon Reference Materials for In Situ Hf Isotope Determination. Geostand. Geoanal. Res. 29 (2), 183–195. https://doi.org/10.1111/j.1751-908X.2005.tb00891.x.
- Wyborn, L.A.I., 1988. Petrology, geochemistry and origin of a major Australian 1880-1840 Ma felsic volcano-plutonic suite: a model for intracontinental felsic magma generation. Precambr. Res. 40–41, 37–60. https://doi.org/10.1016/0301-9268(88) 90060-5.
- Wyborn, L., 1998. Younger ca 1500 Ma granites of the Williams and Naraku Batholiths, Cloncurry district, eastern Mt Isa Inlier: Geochemistry, origin, metallogenic significance and exploration indicators. Aust. J. Earth Sci. 45 (3). https://doi.org/ 10.1080/08120099808728400.
- Wyborn, L.A.I., Page, R.W., McCulloch, M.T., 1988. Petrology, geochronology and isotope geochemistry of the post-1820 Ma granites of the Mount Isa Inlier: Mechanisms for the generation of Proterozoic anorogenic granites. Precambr. Res. 40–41, 509–541. https://doi.org/10.1016/0301-9268(88)90083-6.
- Wyborn, L.A.I., Wyborn, D., Warren, R.G., Drummond, B.J., 1992. Proterozoic granite types in Australia: Implications for lower crust composition, structure and evolution. Earth Environ. Sci. Trans. R. Soc. Edinb. 83 (1–2), 201–209. https://doi.org/ 10.1017/S0263593300007896.
- Wyllie, P.J., 1988. Magma genesis, plate tectonics, and chemical differentiation of the Earth. Rev. Geophys. 26 (3), 370–404. https://doi.org/10.1029/RG026i003p00370.
- Zhao, J.X., Bennett, V.C., 1995. SHRIMP U-Pb zircon geochronology of granites in the Arunta Inlier, central Australia: Implications for Proterozoic crustal evolution. Precambr. Res. 71 (1), 17–43. https://doi.org/10.1016/0301-9268(94)00054-U.
- Zhao, J.X., McCulloch, M.T., 1995. Geochemical and Nd isotopic systematics of granites from the Arunta Inlier, central Australia: Implications for Proterozoic crustal evolution. Precambr. Res. 71 (1), 265–299. https://doi.org/10.1016/0301-9268(94) 00065-Y.
- Zhao, G., Sun, M., Wilde, S.A., Li, S., 2004. A Paleo-Mesoproterozoic supercontinent: Assembly, growth and breakup. Earth Sci. Rev. 67 (1), 91–123. https://doi.org/ 10.1016/j.earscirev.2004.02.003.
- Zhao, X., Seltmann, R., Xue, C., Sun, Q., 2023. Orogenic cyclicity and episodic tectonomagmatic processes in the formation of the Paleozoic northern Yili magmatic arc. Central Asian Orogenic Belt. GSA Bulletin 136 (5–6), 2137–2156. https://doi.org/10.1130/B37192.1.